THESIS

TARGETING SALINITY SOLUTIONS: A NATIONAL GEOSPATIAL FRAMEWORK WITH REGIONAL SALINITY CHARACTERIZATION FOR AGRICULTURAL DESALINATION PLANNING

Submitted by

Kenneth Laffite

Department of Civil and Environmental Engineering

In partial fulfillment of requirements

For the Degree of Master of Science

Colorado State University

Fort Collins, Colorado

Summer 2025

Master's Committee:

Advisor: Ryan Bailey

Ryan Smith
Allan Andales

ABSTRACT

TARGETING SALINITY SOLUTIONS: A NATIONAL GEOSPATIAL FRAMEWORK WITH REGIONAL SALINITY CHARACTERIZATION FOR AGRICULTURAL DESALINATION PLANNING

Water scarcity and rising salinity in agricultural areas present a major threat to the long-term sustainability of irrigation and the quality of water in river systems across the United States. This study aimed to identify suitable locations for implementing desalination technologies to enhance the availability of irrigation water and improve water quality in river systems throughout the contiguous United States, while addressing the insufficient characterization of salinity in these systems. GIS tools, machine learning, a river mass balance approach, and a hydrological model were utilized to generate spatial suitability models and subsequently to characterize salinity in a specific region in greater detail, both temporally and spatially.

For the national assessment, national datasets on watershed boundaries, surface water salinity, groundwater salinity, irrigated lands, cropland cover, solar photovoltaic potential, and wind capacity factor were utilized to characterize watersheds and evaluate their suitability for implementing agricultural desalination powered by renewable energy sources, based on thresholds established in the literature. Several hotspot regions deemed suitable for agricultural desalination were identified, primarily in the western regions of the United States, including parts of the Rocky Mountain states (Colorado, Idaho, Montana, Utah, and Wyoming), most of Texas and Oklahoma in the Southwest, and throughout the Plains region in Kansas, Nebraska, Minnesota, North Dakota, and South Dakota. Additionally, sections of California and Florida, along with the lower Mississippi states. This emphasizes the extensive issues of freshwater

salinization across the country and the potential of agricultural desalination as a source of freshwater.

For one of the suitable regions (Colorado's Lower Arkansas River Valley), a detailed salt mass balance was applied along the river between Pueblo Reservoir in Colorado and Coolidge in Kansas (total distance =317.5 km) to quantify daily groundwater salt ion loadings for the 2000-2020 period, and determine the relative influence of upstream flow, canal diversions, tributary inflow, and groundwater discharge on salt mass within the Arkansas River. Random Forest modeling was used to estimate daily salt ion loads at gaging sites. A SWAT-MODFLOW model was then used to determine the influence of on-farm desalination on groundwater salt loadings to the Arkansas River. Two scenarios were selected: the first with no desalination applied, and the second with half desalination, meaning 50% of the salt ions in the irrigation water are removed. Although agricultural desalination showed no significant impact on the salinity of the river system, this research provides a framework for applying agricultural desalination and establishes a decision-support foundation for managing agricultural water salinity challenges.

ACKNOWLEDGEMENTS

I am deeply grateful for all the experiences and opportunities I gained while pursuing my master's degree at Colorado State University. The insightful guidance provided by my outstanding professors, combined with the collaborative spirit of my classmates, greatly enriched my educational journey. I would like to express my sincere gratitude to my advisor, Dr. Ryan Bailey, for his unwavering support, thoughtful guidance, and welcoming nature. His mentorship was instrumental in the completion of this project and has profoundly shaped my academic and professional growth. I extend my heartfelt thanks to my colleagues, whose valuable feedback, constructive suggestions, and continuous encouragement significantly contributed to the successful execution of my research. This research was generously supported by a grant from the National Science Foundation (NSF) and the INFEWS research group, whose financial assistance made this project possible. Finally, I would like to express my most profound appreciation to my family and friends, whose steadfast support, patience, and encouragement have been invaluable throughout my graduate studies.

TABLE OF CONTENTS

LIST OF TABLES

LIST OF FIGURES

1. INTRODUCTION

1.1 Global Water Scarcity

Despite the appearance of water being an abundant resource, only a small fraction (3%) is freshwater, while most (97%) is salty ocean water. This small fraction must supply the needs of humans and animals, but is often insufficient to meet global demands (Angelakis et al., 2021). Increasing demand, driven by a rising global population, is placing significant pressure on existing resources to meet the water demands of irrigated agriculture, industrial activities, and residential areas (Angelakis et al., 2021; Burn et al., 2015; Khondoker et al., 2023). Furthermore, climate change has a severe impact on water resources. Rising temperatures can exacerbate water scarcity, while changes in weather patterns can alter river flow, impacting irrigation water availability. Furthermore, the likelihood of drought conditions in many regions has increased due to climate change. Likewise, the salinity of irrigation water and agricultural soil severely limits crop production, making salinity a significant concern globally (Khondoker et al., 2023).

1.2 Salinization of Freshwater

Salinity is the chemical term for all the ionic constituents dissolved in water (Wetzel, 2001). It is expressed as the sum of the ionic composition of the major cations and anions present in the water. These constituents include the four major cations Ca^{++}, Mg^{++}, Na^{+}, and K^{+}, and four major anions, HCO_3^{-}, CO_3^{-}, SO_4^{-}, and Cl^{-}. Specific Conductance (SC) has been a prevalent measurement in water quality assessments, routinely recorded at stream-gaging stations by agencies like the U.S. Geological Survey for decades. Specific conductance (also known as electrical conductivity) measures a solution's resistance to electrical flow. The resistance of an aqueous solution to electrical current or electron flow decreases as ion content rises (Wetzel,

2001). The conductance is expressed in Siemens cm^{-1} at 25°C, as per the international chemical standard. The increased concentration of total dissolved solids, which includes the ions mentioned previously, in soil and water is known as salinization.

Salinization is classified as primary if it is the product of natural physical and chemical processes, or secondary if it is the consequence of human activities. Primary salinization can result from soil weathering and the presence of saline parent rocks, where salt is carried and deposited by wind and rain over thousands of years. The causes of secondary salinization are numerous and primarily result from human activities, such as improper land use practices, including poor irrigation, intensive cropping, overgrazing, and deforestation, along with pollution associated with industrialization, including mining, the use of de-icing road salt, and industrial processes outlets. Secondary salinization has been a presence in human history since the earliest human settlements began using irrigation. Early settlers in Mesopotamia, the Indus River Basin, and China were forced to abandon their land and relocate to non-salinized areas due to irrigation-induced secondary salinization. Salt that accumulates in the water table rises to the surface due to increased water infiltration from over-irrigation, dissolving salt back into surface water, and causing salinity. Evapotranspiration leaves dissolved solids behind, which causes salt to accumulate in the soil, becoming a contributing factor to water salinity when flooding or heavy rainfall occurs. Another human action that contributes to water salinity is the inappropriate choice of crops for different soil types. In high waterlogged regions, deep-rooted trees should be used to enhance evapotranspiration and prevent salt from the lower water table, while low water-using crops should be planted in sandy (highly permeable) soil to avoid salt accumulation (Gelburd, n.d.; Ghassemi et al., 1995; Musie & Gonfa, 2023).

1.2.1 Salinization of Irrigated River Systems

Salinity issues in river systems are a growing concern, with significant ecological and economic impacts, particularly affecting agricultural productivity (Thorslund et al., 2021). Irrigation practices, groundwater interactions, climate change, natural processes, and other anthropogenic activities are the leading causes of river salinity. As mentioned previously, irrigation is a significant contributor to freshwater salinization worldwide. Poor irrigation practices can lead to increased saline groundwater levels due to higher irrigation withdrawals. (Custodio, 2002; Thorslund et al., 2021). Excessive salt present in irrigation water can concentrate in the soil through evapoconcentration, leading to soil degradation and the spread of salts to surface and groundwater sources, including rivers. Furthermore, return flows from irrigated agriculture increase the salinity of receiving bodies, like rivers, due to their elevated salt concentrations (Konikow & Person, 1985; Thorslund et al., 2021). In irrigated areas, applied water that is not consumed percolates down to recharge underlying aquifers, eventually providing a return flow of higher salinity water to the river. Excessive irrigation or seepage from canals can result in higher groundwater tables, which can also drive subsurface flows that dissolve salts and minerals from surrounding geological formations, thereby increasing the solute load in the returning water to rivers (Morway & Gates, 2012). Upflux from saline-high water tables under cropped fields, coupled with evaporation, further contributes to soil and potentially river salinity. Certain natural processes, including geological weathering, atmospheric salt deposition, and natural saltwater intrusion, can also impact river salinity. Changes in discharge due to altered precipitation patterns and increased evapotranspiration under climate change can affect the dilution capacity of rivers, potentially leading to increased salinity concentrations.

Besides agriculture, other human activities such as road salt application and mining can also contribute to inland freshwater salinization (Thorslund et al., 2021).

Several river basins worldwide, such as the Mississippi, Ebro, Murray-Darling, Orange, Mekong, Danube, and Rhine, exhibit varying degrees of salinity issues, often linked to agricultural activities. Many sub-basins within these regions exhibit increasing salinization trends or temporarily exceed safe irrigation water-use thresholds, underscoring the widespread nature of this issue. The long-term consequences of ignoring irrigation-water salinity in water management can lead to significant reductions in agricultural profits and overall welfare (Slater et al., 2020; Thorslund et al., 2021).

High concentration of salts in rivers has severe consequences for the economic production of the region, the water quality of the stream, and the health of ecosystems in the river system. Agriculture was previously mentioned as one of the leading causes of water salinization, however, this increased salinity also becomes one of the major concerns for farmers. Increased salinity in the river water diverted for irrigation can negatively impact crop yield (Khondoker et al., 2023; Morway & Gates, 2012; Munns, 2002). This is due to high salt concentrations in the soil solution increasing osmotic potential, making it harder for plants to absorb water, potentially leading to dehydration and death (Galvani, 2007; Khondoker et al., 2023). The need for additional water to leach accumulated salts from the root zone also increases with higher irrigation water salinity (Ben-Gal et al., 2009; Kumar et al., 2017). Moreover, increased salinity can make river water less suitable for various uses, including drinking water and industrial purposes. Increased salinity also affects river biota, impacting species richness, abundance, functional traits, and ecosystem processes. If the salinity exceeds the tolerance levels of aquatic organisms, it can lead to increased mortality rates and altered growth and

photosynthesis (Khondoker et al., 2023; Thorslund et al., 2021). Lastly, as mentioned previously, using saline river water for irrigation contributes to soil salinization, which deteriorates soil structure, reduces water infiltration, and increases the risk of soil erosion. Therefore, managing salinity in river systems requires an integrated approach that considers irrigation practices, groundwater interactions, natural influences, and the potential impacts of climate change, alongside the implementation of appropriate monitoring and mitigation strategies.

1.2.2 Alternatives to Address Salinity

Several ways for addressing salinity issues have been proposed and implemented in irrigated river systems. The improvement of irrigation management has been targeted by implementing more efficient irrigation practices to reduce water withdrawals and return flows, thereby limiting salt loading into the river systems. Also, managing leaching requirements based on irrigation water salinity and crop tolerance is crucial. Effective drainage systems are crucial in preventing the accumulation of saline groundwater and facilitating the removal of excess salts from irrigated lands (Kaner et al., 2017; Kumar et al., 2017; Morway & Gates, 2012). Investments in salinity control projects, such as those implemented in the western United States, aim to manage and mitigate salinity problems in irrigated stream-aquifer systems (Konikow & Person, 1985). Given these challenges, alternative water supplies for agriculture are essential; therefore, desalination has been recognized by the Intergovernmental Panel on Climate Change (IPCC) as a potential strategy to assist agriculture in adapting to the impacts of climate change, particularly in arid or semi-arid regions (Angelakis et al., 2021; Khondoker et al., 2023). Desalination of brackish water or even river water with high salinity could provide a freshwater source, reducing reliance on saline river water for irrigation, although costs and brine disposal need consideration (Abu El-Maaty et al., 2023; Barron et al., 2015; Kumar et al., 2017).

Furthermore, long-term monitoring of salinity levels in rivers is crucial for understanding trends and the effectiveness of management strategies (Thorslund et al., 2021).

1.2.3 Desalination: A Strategy Worth Exploring

Desalination is currently used in over 150 countries worldwide. Key countries employing desalination include Algeria, Libya, Egypt, Tunisia, and Morocco in Africa, as well as China, Japan, Saudi Arabia, Kuwait, the United Arab Emirates, Qatar, Bahrain, Oman, and Israel in Asia. Countries like Kuwait, Qatar, and Malta obtain more than half of their water supply from desalination. The primary users of desalinated water for irrigation are Kuwait, the United Arab Emirates, Cyprus, Israel, and Qatar. Although the cost of desalination is decreasing, it remains beyond the economic means of most impoverished countries facing water shortages due to its highly energy-intensive nature. Research focuses on finding more cost-effective and technically feasible desalination methods that can be applied at various economic levels to address the growing water crisis (Musie & Gonfa, 2023). For these reasons, desalination powered by renewable energy sources is a potentially appealing option. Unfortunately, saline water resources are not well characterized in many regions, which hinders the consideration of such technologies (Androwski et al., 2011).

1.2.4 Spatially Characterizing Saline Water Resources

Due to the spatial distribution of water resources and irrigated agriculture, Geographic Information Systems (GIS) are widely employed to characterize salinity in various ways, aiding in its assessment, monitoring, and management. Visualization and spatial mapping are primary uses of GIS, which facilitate the creation of maps that depict the spatial distribution of salinity in soils and water. GIS enables the classification of salinity levels based on predefined thresholds and the generation of thematic maps that illustrate distinct zones of varying salinity levels.

Furthermore, GIS acts as a platform for integrating diverse datasets related to salinity, allowing for combined analyses that include remotely sensed imagery, field measurements of soil and water salinity, topographical information, geological data, land use data, and climate information (Amer, 2021; Eldeiry & Garcia, 2004; Garcia et al., 2006; Gojiya et al., 2023; Metternicht, 2001). GIS also offers a platform for spatial salinity analysis alongside other environmental factors, including overlay analysis, change detection analysis, and geostatistical analysis (Amer, 2021; Metternicht, 2001). Similarly, GIS serves as a framework for developing and implementing models to predict salinity and its impacts. It facilitates the integration of spatial variable parameters into models that simulate the movement of water and salt. Using fuzzy logic-based systems within GIS tools allows for the assessment of the likelihood, nature, and magnitude of salinity changes. Data for machine learning models can be prepared in GIS tools for predictions based on various spatial explanatory variables and mapped back into GIS for visualization and analysis. (Eldeiry & Garcia, 2004; Garcia et al., 2006; Knierim et al., 2020; Metternicht, 2001). By providing comprehensive spatial information on salinity, GIS supports informed decision-making regarding land management, irrigation practices, and salinity control and reclamation efforts. Visualizing salinity distribution, analyzing its relationships with other factors, and predicting future scenarios make GIS a valuable tool for stakeholders and decision-makers.

Furthermore, efforts like (Thorslund & van Vliet, 2020) have focused on collecting global salinity data for surface water and groundwater to create a worldwide database; however, they have not categorized the data or regions in any form. (Amer, 2021) investigated how poor-quality irrigation water and waterlogging are spatially linked and contribute to the decline of farmland in dry regions, while (Garcia et al., 2006) focused on crop yield reduction. Others have

examined the availability of saline water resources in areas suitable for renewable energy-powered desalination, as in (Androwski et al., 2011) , who investigated the co-location of saline groundwater availability and suitable wind power resources in the contiguous United States. This opens the door for expanding on research by targeting the characterization of salinity in groundwater and surface water in irrigated areas with potential for multiple sources of renewable energy to power desalination technologies.

1.2.5 Long-term Monitoring of Salinity

The importance of long-term monitoring of areas with salinity issues has been previously stressed. This is due to several factors often mentioned in the literature, including understanding historical trends, calibration and validation of models, the impact of human activities, and assessment of management strategies. First, understanding historical trends and variations in salinity requires long-term data collection, as short-term monitoring can lead to erroneous projections and a misunderstanding of the water system's dynamics (Cunillera-Montcusí et al., 2022; Konikow & Person, 1985; Thorslund et al., 2021). The study by (Konikow & Person, 1985) highlights this point. Their initial model predictions of long-term salinity increase proved inaccurate because the calibration period captured a short-term trend that was not representative of the long-term pattern. Second, long-term monitoring is crucial for evaluating the long-term effects of human activities, such as irrigation, on freshwater salinization over extended periods. Without long-term data, it is difficult to distinguish between short-term fluctuations and long-term trends driven by human activities (Thorslund et al., 2021). Third, evaluating the long-term effectiveness and sustainability of water management strategies, including desalination, necessitates continuous monitoring (Angelakis et al., 2021; Ghermandi et al., 2014; Slater et al., 2020; Yermiyahu et al., 2007). This is important because identifying long-term performance and

challenges for desalination plants, which are expected to operate for decades, will help ensure they achieve their intended goals. Fourth, long-term data sets are vital for calibrating and validating models that aim to predict future water quality and available resources (Konikow & Person, 1985; Thorslund et al., 2021). Finally, long-term soil and water salinity monitoring is important for understanding its cumulative effects on crop productivity and soil health (Khondoker et al., 2023; Morway & Gates, 2012; Munns, 2002; Thorslund et al., 2021).

1.3 Machine learning and Random Forest in water quality modeling

Machine Learning (ML), a subset of artificial intelligence, is defined as the science of programming computers to learn from data (Géron, 2022). It involves the examination of data to identify trends, patterns, and rules, and represent relationships between input and output variables (Nasir et al., 2022; Nouraki et al., 2021). Classification and regression (prediction) are the two common tasks ML models perform. ML models can be classified according to how they are supervised during training. In supervised ML models, such as Random Forest, the training data fed to the model includes the desired solutions. Random Forest (RF) is an ensemble of decision trees that outputs the average forecast of all trees to provide a final prediction (Breiman, 1996; Géron, 2022; Ho, 1995).

Their nonlinear structure, ability to identify complicated events, handling diverse datasets, and handling missing data are advantages that have enabled the increasing and practical application of machine learning models in various aspects of water quality studies (Behrouz et al., 2022; Melesse et al., 2020; Mokhtar et al., 2022; Nasir et al., 2022). Applications of ML models in water quality are as follows: modeling and predicting water quality parameters such as surface water salinity via electrical conductivity, concentrations of total dissolved solids, total nitrogen, total phosphorus, pH, dissolved oxygen, sodium adsorption ratio, and total hardness in

streams, lakes, and irrigation water (Ali Khan et al., 2022; Alnahit et al., 2022; Behrouz et al., 2022; Jena et al., 2022; Melesse et al., 2020; Nasir et al., 2022; Nouraki et al., 2021). Other applications include classification and forecasting of water quality to categorize water quality into different classes, to predict a water quality index, a metric that quantifies overall water quality, or the identification of the most influential variables affecting it (Mokhtar et al., 2022; Nasir et al., 2022; Shams et al., 2024).

Random Forest has been applied to several of the applications described previously, including the prediction of water quality parameters related to salinity (Ali Khan et al., 2022). This is due to its high prediction accuracy in regression tasks related to water quality (Nouraki et al., 2021; Shams et al., 2024; Tyralis et al., 2019). The model exhibits less susceptibility to overfitting compared to other machine learning algorithms (Behrouz et al., 2022). Additionally, it can handle non-linear relationships without requiring any explicit specification of these relationships (Harrison et al., 2021). For these reasons, machine learning models, particularly Random Forest, have become valuable tools in water quality studies, increasing their adoption in the field.

1.4 Objectives

The increased concern about salinity issues in river systems, which affect agricultural productivity, has been previously emphasized. Thus, in this study, we have two main objectives:

1. ***Identify salinity-impaired regions in the contiguous United States (CONUS) that have the potential to utilize renewable energy-powered desalination to mitigate the environmental and economic impacts of freshwater salinization***. To achieve this, we developed a geospatial workflow to characterize watersheds using data derived from national

datasets and assess their suitability for the application of desalination technologies powered by renewable energy, based on thresholds established in the literature.

2. ***Evaluate the effectiveness of on-farm desalination for a salinity-impaired river valley***. The Lower Arkansas River in southeastern Colorado was chosen as a case study because it is one of the most saline rivers in the United States, as is identified as a suitable region for desalination, based on results from Objective 1. To achieve this, we applied a salt ion mass balance model to the Arkansas River between Pueblo Reservoir and the Colorado-Kansas state line (total river length = 317.5km) for the 2000-2020 period, using a Random Forest machine learning model to estimate daily salt ion concentrations and salt ion loads at gage sites, thereby allowing the estimation of groundwater salt loading to the river. Subsequently, a SWAT-MODFLOW-Salt model of a sub-region was used and extrapolated to evaluate the application of desalination on the river system.

2. IDENTIFY SUITABLE LOCATIONS WITHIN THE CONUS FOR RENEWABLE ENERGY-POWERED AGRICULTURAL DESALINATION

2.1 Methodology

This section outlines the methodology for identifying locations in the conterminous United States that are suitable for applying desalination technologies to enhance irrigation water availability. To achieve the first objective of this thesis, which is to develop a geospatial method for identifying salinity-impaired regions in the contiguous United States (CONUS) that could benefit from renewable energy-powered desalination to mitigate the environmental and economic impacts of freshwater salinization, we developed a geospatial workflow in ArcGIS Pro. This workflow characterizes watersheds using data derived from national GIS datasets and evaluates their suitability for implementing desalination technologies powered by renewable energy based on thresholds established in the literature. To determine the location of these watersheds, several spatial datasets were gathered and processed in ArcGIS Pro (see Table 1).

Table 1: Dataset information for layers used in the GIS workflow.

Layer name	Data set	Source	Format
Contiguous US Boundary	United States State Boundaries	ESRI	Esri File Shapefile
HUC12 Watersheds	USGS Watershed Boundary Dataset (WBD)	U.S. Geological Survey	Esri File GeoDatabase
Groundwater Salinity Measurements	Geochemical Database for the Brackish Groundwater Assessment of the United States: Dissolved-Solids Dataset	U.S. Geological Survey	Esri File GeoDatabase
Irrigated Lands	LANID HRU HUC12 intersected feature classes 2000-20	U.S. Geological Survey	Esri File GeoDatabase
Surface Water Salinity Measurements	Water Quality Portal (WQP)	National Water Quality Monitoring Council (EPA and USG)	Tabular XY dataset
Cropland Cover	2022 Cropland Data Layer	United States Department of Agriculture (USDA)	GEOTIFF raster
Solar PV Potential Output	Long-term yearly average of Potential photovoltaic electricity production – USA - Global Solar Atlas 2.0	The World Bank	GEOTIFF raster
Wind Capacity Factor	Wind Power Class - Onshore	The World Bank	GEOTIFF raster

This workflow was coded in the ArcPy Python library for ease of reproducibility and sharing; the code is included in the support material of this thesis.

2.1.1 Data collection and preprocessing

The Contiguous US Boundary layer, which defines the study region, was confined to the contiguous United States via the *United States State Boundaries* layer from ESRI. This shapefile was used to standardize the spatial extent of all layers. Additionally, hydrologic units (HU) were selected as the primary spatial unit, layer HUC12 Watersheds, due to their relevance to water resource management and to facilitate later modeling analyses. They are the areal extent of surface water drainage to an outlet (Jones et al., 2022). The hydrologic unit code (HUC) divides and subdivides HUs based on surface features. HUCs are identified by numerical classifiers, which include 2-, 4-, 8-, 10-, or 12-digit codes, with the latter representing the smallest subdivision. HUC12, the most detailed HU discretization available from the dataset, was used. Attributes from all datasets considered were assigned to each HUC12 watershed for the assessment. The HUC12 feature class layer was extracted from the USGS Watershed Boundary Dataset (WBD) GeoDatabase file by the USGS (Jones et al., 2022). This dataset consists of hydrologic unit data that aligns with the national criteria for delineation and resolution. Furthermore, information on the Irrigated Lands layers, see Figure 1, originates from the USGS's *LANID HRU HUC12 intersected feature classes 2000-20* (Donald Martin et al., 2024). This dataset utilizes the Landsat-based Irrigation Dataset (LANID) to pinpoint the locations of irrigated croplands (Xie & Lark, 2021). HUC12s that contain irrigated lands were identified using this dataset.

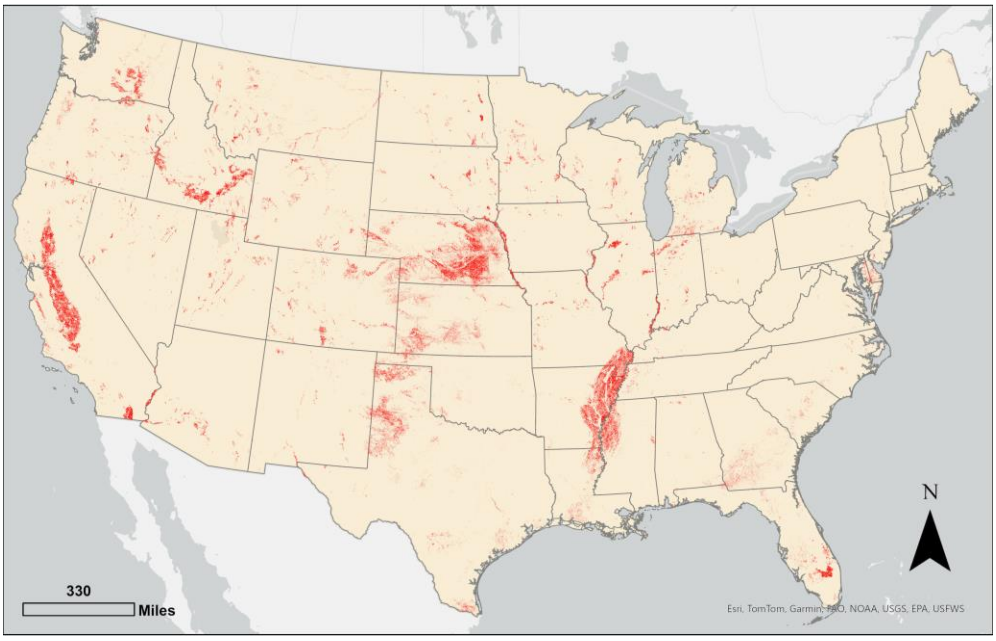

Figure 1: The irrigated lands layer contains every irrigated field within the CONUS highlighted in red. The map is composed of polygons representing individual irrigated fields.

Data on groundwater specific conductance, for the Groundwater Salinity Measurements layer, were sourced from the *Geochemical Database for the Brackish Groundwater Assessment of the United States: Dissolved-Solids Dataset* (Stanton et al., 2017), see Figure 2B. Sampling for this dataset was conducted in microSiemens per centimeter at 25 degrees Celsius from sampling wells across the United States, which contain geographic location coordinates and well-depth measurements. Specific conductance was used as a proxy for salt concentration in groundwater. Specific conductance is an easily measured and practical index of the total concentration of ionized solutes in an aqueous sample. On the other hand, the National Water Quality Monitoring Council's *Water Quality Portal (WQP)* was used to gather specific conductance data for surface water sources, which are used in the Surface Water Salinity Measurements layer (see Figure 2A). This data can also serve as a proxy for salt concentrations in surface water. (Read et al., 2017) states that the WQP was developed by the U.S. Environmental Protection Agency (EPA), the

U.S. Geological Survey (USGS), and the National Water Quality Monitoring to provide a single point of access for standardized water quality data from groundwater, inland, and coastal waters.

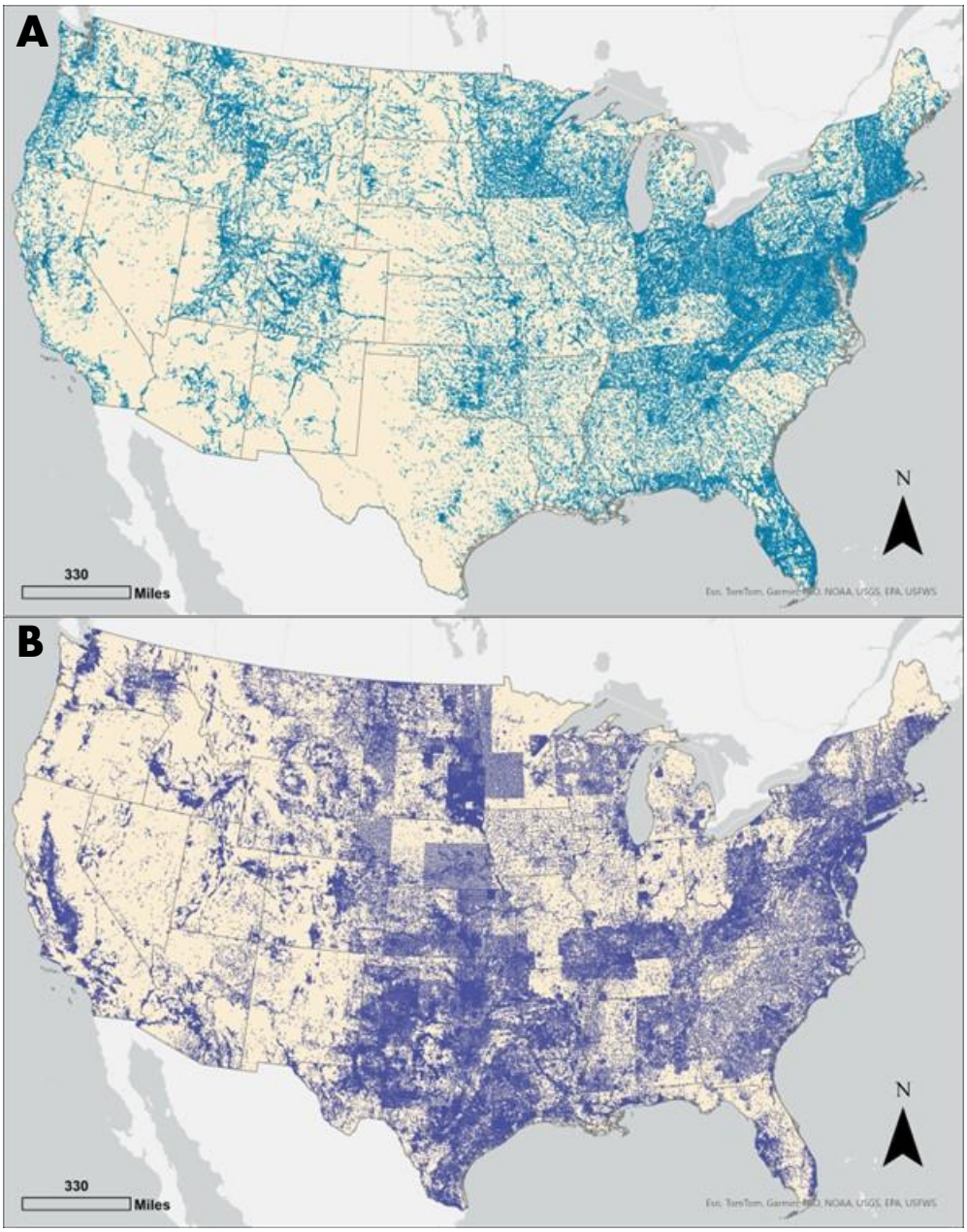

Figure 2: Specific conductance points measurements for (A) surface water sources and (B) groundwater sources. Each dot in the map represents a SC measurement in either surface or groundwater.

Crop-specific land cover data were gathered from the US Department of Agriculture (USDA) *2022 Cropland Data Layer.* The Cropland Data Layer is a high-resolution (30-meter)

geo-referenced land cover map of crops grown throughout the United States (Boryan et al., 2011). This dataset was used to identify the types of crops grown in each HUC12 watershed. Additionally, photovoltaic power output (PVOUT) data were obtained from the Global Solar Atlas to evaluate the feasibility of solar energy for desalination in the study area; see Figure 3. PVOUT is the power output achievable by a typical PV system by converting available solar resources to electric power, considering the impact of air temperature, terrain horizon, albedo, and factors affecting system performance such as module tilt, configuration, and shading (Suri et al., 2020). PVOUT is measured in kilowatt-hours per installed kilowatt peak (kWh/kWp), which represents the amount of power generated per unit of installed PV capacity over the long term, also known as the specific yield. Finally, the capacity factor is a measure of the annual energy yield of a wind turbine, expressed as a ratio of the energy produced over the energy that would

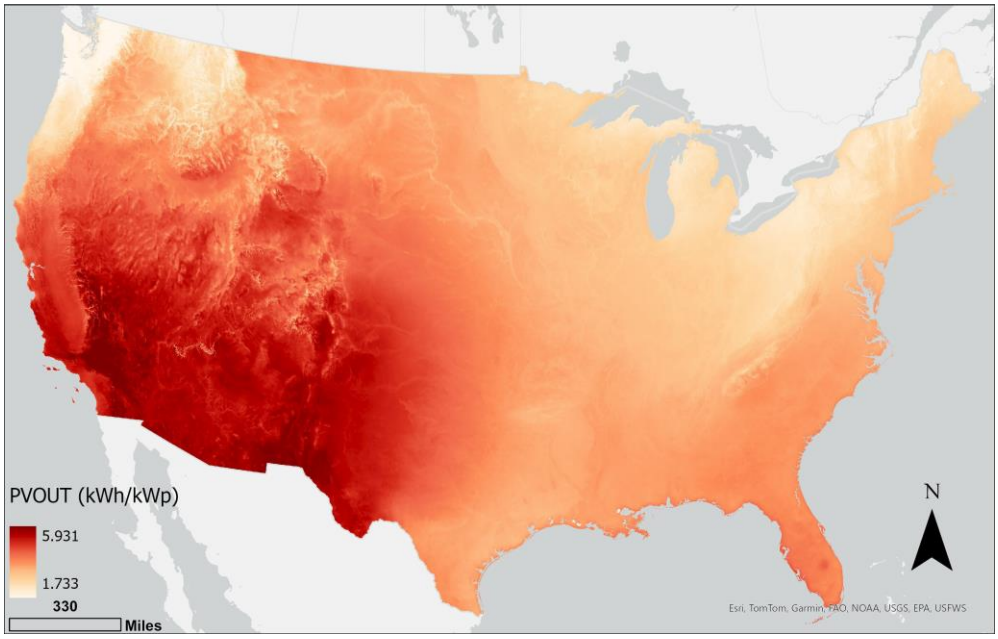

Figure 3: Solar photovoltaic output (PVOUT) for the CONUS in kWh/kWp. Higher PVOUT values indicate a greater potential for solar-powered energy generation.

be produced if the wind turbines were operated at rated power throughout the year (Davis et al., 2023). Higher capacity factors indicate higher annual energy yield. The wind power capacity

factor raster dataset was sourced from the *Global Wind Atlas* (see Figure 4), specifically the IEC Class III capacity factor layer, which considers turbines that generate the most energy at lower speeds (Davis et al., 2023).

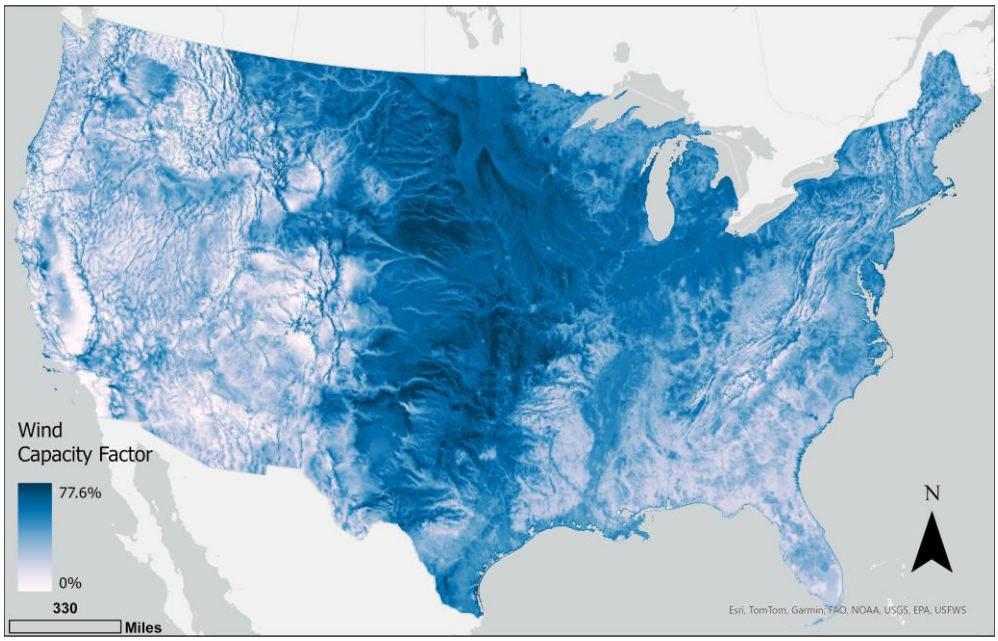

Figure 4: Wind capacity factor (CF) for the CONUS. Higher CF values indicate a greater potential for wind-powered energy generation.

2.1.2 ArcGIS Workflow

All previously described datasets were imported into a newly created ESRI geodatabase file for further processing, ensuring that all spatial data were stored in a centralized location for efficient analysis, as detailed in Figure 5. Subsequently, each dataset was standardized to maintain consistency in spatial extent and coordinate reference system. The USA Contiguous Albers Equal Area Conic projection (EPSG: 102039) was applied to all datasets to minimize distortion in area calculations. Maps were created using North American Datum 1983 and were projected in Albers Equal Area Conic to preserve spatial dimensions for calculations. The Albers Equal Area Conic projection is suited for the conterminous U.S. and has a 1.25% maximum scale distortion between 29°30’N and 45°30’N (Syner, 1987). Raster and vector datasets that did not

conform to this projection were reprojected using the ArcGIS *Project* and *Project Raster* tools. To ensure that only the geographic areas of the study were included, datasets were clipped to the contiguous U.S. boundary using the *Clip* tool. This tool facilitated the removal of spatial data outside the study area, reducing computational load and maintaining analytical focus.

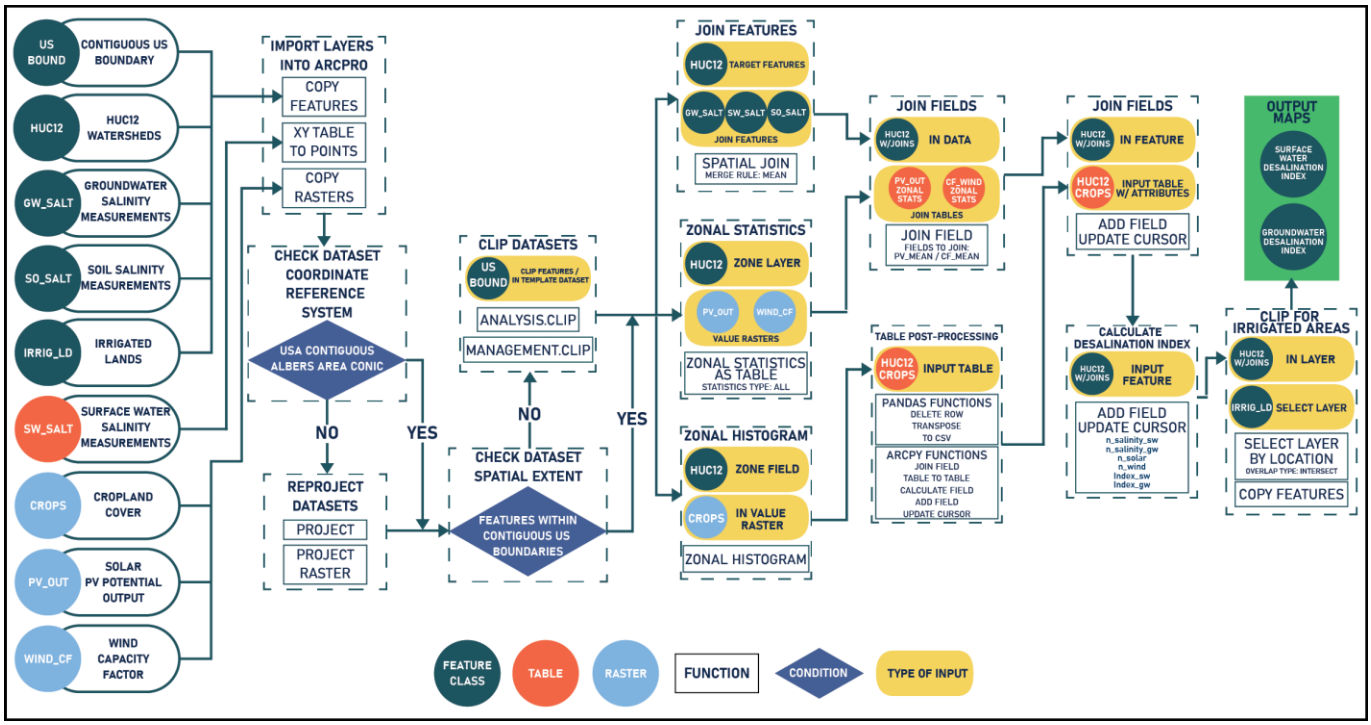

Figure 5: ArcGIS Pro workflow used to determine agricultural desalination suitable regions. The workflow was coded in the ArcPy Python library for ease of reproducibility.

As previously mentioned, HUC12 watersheds were selected as the spatial unit for the analysis. As a result, attribute data from the other layers was aggregated within these watershed boundaries. Spatial joins were used for surface water and groundwater specific conductance point measurements. When more than one measurement was recorded within a HUC12, the average was considered. Similarly, the *Zonal Statistics* tool was used to compute the mean photovoltaic power output and the mean wind power capacity factor for renewable energy potential for each HUC12. Furthermore, the *Zonal Histogram* tool was used to determine the types of crops grown in each HUC12 from the cropland cover layer. This tool provided a table

with the HUC12s containing production for every crop type considered. Further processing using Pandas functions for deleting rows, transposing the table, and exporting to CSV; see detailed code in the support materials. Subsequently, the *Add Field* and *Update Cursor* tools were used to aggregate the crop type attributes into each HUC12 watershed.

To assess the feasibility of desalination technologies, suitability indices for salinity and renewable energy were established based on classifications found in the literature. Table 2 details the ranges used to determine the respective desalination index (DI) multipliers for each category. Surface and groundwater salinity suitability were classified by the degree of restriction into severe, slight to moderate, and no restriction from their average specific conductance value (Ayers & Westcot, 1985). Based on the average photovoltaic power output (PVOUT), solar output potential was ranked as excellent, mid-range, and lower potential (Suri et al., 2020).

Table 2: Index Multipliers based on HUC12 watershed properties used for the DI calculation.

Degree of restriction	**Specific Conductance (dS/m)**	**Salinity Suitability Index Multiplier (n_{salt})**
Severe restriction	≥ 3.0	1.0
Slight to moderate restriction	0.7 < SC < 3.0	0.5
No restriction	≤ 0.7	0

Solar output potential	**PVOUT (kWh/kWp)**	**Solar Suitability Index Multiplier (n_{pv})**
Excellent potential	≥ 4.5	1.0
Mid-range potential	3.5 < PVOUT < 4.5	0.5
Lower potential	≤ 3.5	0

Wind power suitability	**Capacity factor (%)**	**Wind Suitability Index Multiplier (n_{cf})**
Highly suitable	≥ 0.4	1.0
Moderately suitable	0.2 < CF < 0.4	0.5
Unsuitable	≤ 0.2	0

Due to the lack of a standardized classification of wind power for capacity factors, several sources were considered for the classification, landing on highly suitable, moderately suitable, and unsuitable (Davis et al., 2023; *Wind Energy Factsheet | Center for Sustainable Systems*, 2024; Wiser et al., 2023).

Equation (1) was used to determine the Desalination Index (*DI*) for surface water and groundwater sources from the Index multipliers described previously. The salinity suitability index multiplier (n_{salt}) is doubled for HUC12s with a higher salinity impairment, which are prioritized in the analysis. Subsequently, the maximum value of the solar suitability index multiplier (n_{pv}) and wind suitability index multiplier (n_{cf}) is added to n_{salt}. The result is multiplied by one-third to obtain the Desalination Index (*DI*), between 0 and 1. A higher *DI* indicates a greater suitability for applying desalination technologies powered by renewable energy sources.

$$DI = \frac{1}{3}\left(2 \times n_{salt} + max\left(n_{pv}, n_{cf}\right)\right) \quad (1)$$

Finally, after computing the desalination indices, results were visualized in color-coded maps to illustrate the spatial variation in desalination feasibility across the contiguous United States. HUC12s were classified according to their DI values into higher suitability, moderate suitability, and lower suitability, as described in Table 3.

Table 3: HUC12 Watersheds Classification based on Desalination Index values.

HUC12 Suitability	Desalination Index (DI)
Higher Suitability	1
Moderate Suitability	0.83
Moderate Suitability	0.67
Lower Suitability	0.5

2.2 Results

Several areas suitable for desalination applications were identified through the analysis detailed in the previous section. The eight-region division from the Bureau of Economic Analysis, as shown in Figure 6, was utilized for a clearer description of the results. HUC12 watersheds with potential for surface water desalination in the CONUS are illustrated in Figure 7. All the Rocky Mountain states have surface waters impaired by salinity. Montana and Wyoming show the greatest extent of affected HUC12 watersheds. However, in Colorado, particularly in the South Platte River and Arkansas River watersheds, some areas demonstrate high suitability, while others show moderate suitability. Similarly, many watersheds in northern Utah demonstrate high suitability, especially those surrounding the Great Salt Lake.

Figure 6: Map of the United States with the Bureau of Economic Analysis's eight-region subdivision

Higher suitability areas are located in Texas, Oklahoma, and New Mexico, with a lesser extent in the Southwest region. Oklahoma shows an almost uniform distribution of higher suitability areas across most of the state, with over 31% of the state's total extension deemed suitable (see Table 4). A similar scenario occurs in Kansas, where over 22% of its total area, in the Plains region, is classified as moderate suitability areas. Additionally, several watersheds of the Missouri River and its tributaries in North Dakota, South Dakota, and Nebraska exhibit moderate suitability as well. All states in the Great Lakes region include watersheds with moderate suitability. Conversely, Florida stands out as the only state in the Southwest region with a significant number of watersheds that have a higher or moderate level of suitability, accounting for more than 17% of the state's area. A similar situation can be observed in

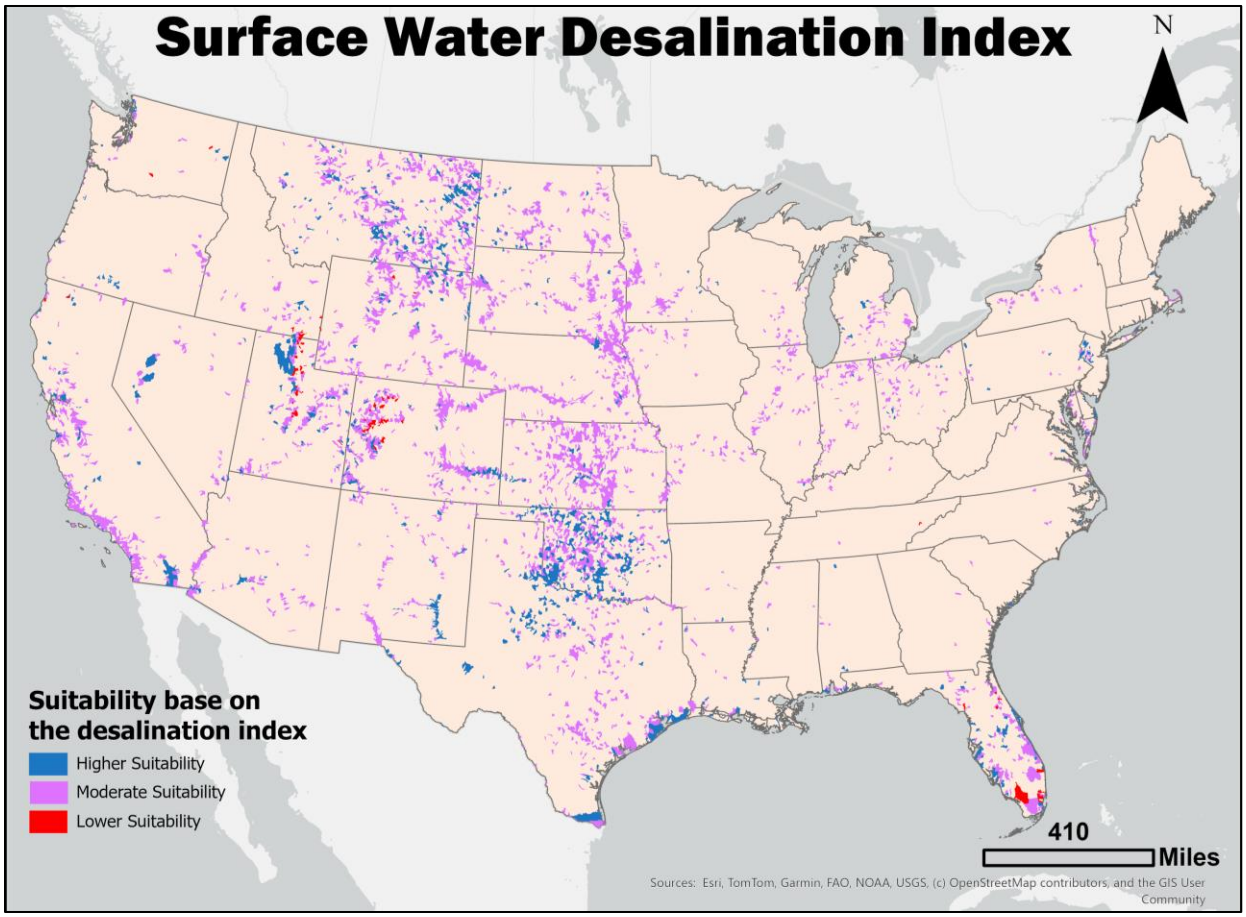

Figure 7: Surface Water Desalination Index map highlighting HUC12 watersheds deemed suitable for agricultural desalination from surface water sources.

California, which accounts for over 9% of the state's total area, in the Far West region, where several watersheds with moderate to high suitability are situated in the Central Valley, along the coast north of Los Angeles, and further south, at the borders with Mexico and Arizona.

Table 4: Percentage of each state's total area deemed suitable for agricultural desalination with surface water sources. Scale bars in yellow indicate relative watershed coverage when compared to the rest of the states.

	AL	AZ	AR	CA	CO	CT	DE	DC	FL	GA
High	0.65%	0.53%	0.13%	1.72%	2.18%	0.00%	5.15%	0.00%	4.28%	0.00%
Moderate	0.59%	2.84%	0.76%	7.58%	12.76%	0.00%	2.38%	0.00%	10.89%	0.36%
Low	0.00%	0.00%	0.00%	0.05%	1.05%	0.00%	0.00%	0.00%	2.74%	0.00%
	ID	**IL**	**IN**	**IA**	**KS**	**KY**	**LA**	**ME**	**MD**	**MA**
High	0.39%	0.06%	0.07%	0.00%	1.68%	0.00%	1.13%	0.00%	1.10%	0.68%
Moderate	2.32%	5.04%	7.07%	3.89%	19.89%	0.73%	2.20%	0.00%	4.76%	1.99%
Low	0.37%	0.00%	0.00%	0.00%	0.00%	0.00%	0.00%	0.00%	0.00%	0.00%
	MI	**MN**	**MS**	**MO**	**MT**	**NE**	**NV**	**NH**	**NJ**	**NM**
High	0.53%	0.11%	0.25%	0.07%	5.16%	0.63%	1.18%	0.51%	7.18%	1.26%
Moderate	4.00%	4.26%	0.57%	3.30%	12.72%	13.03%	1.80%	0.00%	2.25%	3.57%
Low	0.00%	0.00%	0.00%	0.00%	0.00%	0.00%	0.00%	0.00%	0.00%	0.00%
	NY	**NC**	**ND**	**OH**	**OK**	**OR**	**PA**	**RI**	**SC**	**SD**
High	0.10%	0.08%	1.40%	0.35%	15.63%	0.42%	0.52%	0.00%	0.15%	0.93%
Moderate	2.78%	0.42%	8.60%	5.58%	15.59%	1.37%	0.74%	0.00%	0.16%	13.96%
Low	0.00%	0.00%	0.00%	0.00%	0.00%	0.00%	0.00%	0.00%	0.00%	0.00%
	TN	**TX**	**UT**	**VT**	**VA**	**WA**	**WV**	**WI**	**WY**	
High	0.00%	3.32%	4.82%	0.00%	0.33%	0.54%	0.00%	0.08%	1.67%	
Moderate	0.10%	5.41%	8.41%	4.16%	1.01%	0.89%	0.00%	1.92%	12.31%	
Low	0.08%	0.00%	1.09%	0.00%	0.00%	0.16%	0.00%	0.00%	0.15%	

On the other hand, Figure 8 shows the HUC12 watersheds with groundwater desalination potential for the CONUS. In general, the same regions highlighted for surface water sources exhibited similar or greater suitability for desalination. Again, all states in the Rocky Mountain region display moderate to high suitability but encompass a larger number of watersheds. A similar situation arises in the Southwest region, particularly in Texas; however, it sees the most significant increase in watersheds across the entire CONUS, with nearly 48% of its total area considered suitable for agricultural desalination (see Table 5). For the Plains region, a similar case arises as in the Rocky Mountain region, where the number of watersheds in the same areas

along the Missouri River increases. Additionally, nearly half (47%) of the state of Kansas displays at least moderate suitability. California's Central Valley is experiencing an increase in the number of watersheds with moderate suitability in the Far West region, covering 17.3% of the entire state. Meanwhile, Nevada's western side also now displays numerous watersheds with moderate or higher suitability. For the Great Lakes region, again, all states contain several watersheds with moderate suitability.

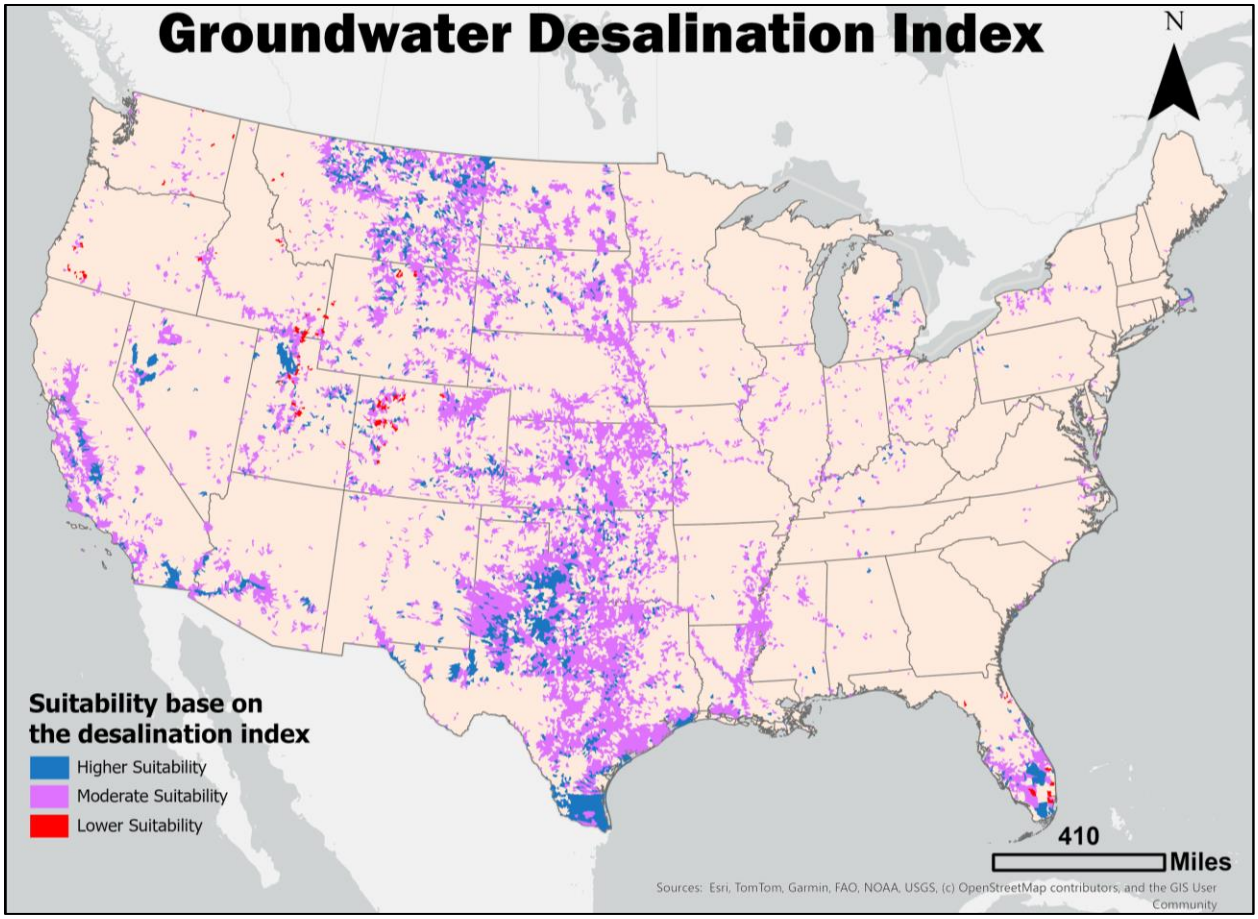

Figure 8: Groundwater Desalination Index map highlighting HUC12 watersheds deemed suitable for agricultural desalination from groundwater sources.

The Southeast, however, shows significant changes as more states now possess watersheds with moderate suitability for desalination. Florida has a significant number of watersheds, mostly found in its southern region, with a growing number of higher suitability

locations accounting for nearly 22.5% of its total area. The most notable difference, however, is in the states along the lower Mississippi River compared to the previous scenario with surface water sources. Arkansas, Mississippi, and Louisiana show several moderately suitable watersheds along the Mississippi River.

Table 5: Percentage of each state's total area deemed suitable for agricultural desalination with groundwater sources. Scale bars in green indicate relative watershed coverage when compared to the rest of the states.

	AL	AZ	AR	CA	CO	CT	DE	DC	FL	GA
High	0.20%	2.22%	0.18%	3.13%	3.62%	0.00%	0.00%	0.00%	6.38%	0.00%
Moderate	1.48%	8.39%	10.92%	14.16%	18.98%	0.49%	3.35%	0.00%	14.04%	0.00%
Low	0.00%	0.00%	0.00%	0.00%	1.34%	0.00%	0.00%	0.00%	1.53%	0.00%
	ID	**IL**	**IN**	**IA**	**KS**	**KY**	**LA**	**ME**	**MD**	**MA**
High	0.17%	0.11%	0.08%	0.12%	2.91%	1.17%	1.08%	0.00%	0.27%	1.99%
Moderate	7.29%	5.38%	4.37%	7.63%	44.47%	3.09%	21.02%	0.14%	2.56%	2.74%
Low	0.99%	0.00%	0.00%	0.00%	0.00%	0.00%	0.00%	0.00%	0.00%	0.00%
	MI	**MN**	**MS**	**MO**	**MT**	**NE**	**NV**	**NH**	**NJ**	**NM**
High	1.19%	0.08%	0.34%	0.30%	8.77%	0.72%	2.22%	0.00%	1.04%	1.83%
Moderate	4.42%	7.32%	9.62%	8.22%	23.92%	20.81%	5.80%	0.00%	1.58%	7.91%
Low	0.00%	0.00%	0.00%	0.00%	0.08%	0.00%	0.00%	0.00%	0.00%	0.00%
	NY	**NC**	**ND**	**OH**	**OK**	**OR**	**PA**	**RI**	**SC**	**SD**
High	0.25%	0.00%	3.08%	0.15%	8.90%	0.14%	0.44%	0.00%	0.13%	3.18%
Moderate	4.19%	1.83%	21.09%	4.92%	36.36%	2.98%	1.08%	0.00%	0.47%	25.33%
Low	0.00%	0.00%	0.00%	0.00%	0.00%	0.58%	0.00%	0.00%	0.00%	0.00%
	TN	**TX**	**UT**	**VT**	**VA**	**WA**	**WV**	**WI**	**WY**	
High	0.13%	11.68%	5.08%	0.00%	0.00%	0.04%	0.00%	0.07%	2.96%	
Moderate	1.38%	36.27%	11.21%	0.09%	1.19%	2.78%	1.13%	1.72%	18.44%	
Low	0.00%	0.00%	1.16%	0.00%	0.00%	0.34%	0.00%	0.00%	0.52%	

2.3 Discussion

To my knowledge, there are not many studies in the literature that have attempted this kind of work or something similar. Perhaps the closest example is (Androwski et al., 2011), who examined the desalination potential of groundwater while focusing on wind energy as a renewable energy source. When compared to the Groundwater Desalination Index map (Figure 8) presented in this thesis, most of the regions identified by Androwski, et al. overlap with areas deemed suitable in this thesis. The Plains and the Rocky Mountain regions' aquifers are the most

significant regions identified by Androwski, et al. as containing both saline groundwater and sufficient wind resources; likewise, a considerable number of watersheds were signaled as at least moderately suitable in this study. Furthermore, both studies highlight areas in Texas, Iowa, Illinois, and New York to different extents, however. This disparity in results is likely to be due to the different nature of the results. While Androwski et al. focus solely on the aquifers in the regions mentioned with wind-powered resource potential, the methodology of this study includes solar-powered resource potential and irrigated lands at a smaller spatial unit (HUC12 watersheds). Additionally, we considered surface water resources, which are prevalent in irrigated agriculture, therefore increasing the scope of the study.

The potential of desalination to address water stress has been previously emphasized, alongside the insufficient characterization of salinity in various regions. This study lays the groundwork for further research by identifying regions that are suitable for implementing these technologies. Additionally, the scope is narrowed to a specific spatial unit, allowing for flexibility in future research to consider larger watersheds within the HUC classification. It is worth noting that these results should be regarded as preliminary and provide an opportunity for further investigation of the highlighted watersheds. The complexity associated with various types of irrigation systems, water sources, desalination technologies, and renewable energy sources makes each area a unique case study. Moreover, other factors not addressed, such as the economic and regulatory feasibility of implementing these technologies, along with new government incentives and the willingness of irrigators to adopt these measures, should be factored into a more comprehensive analysis. This can create opportunities to advance this work with more detailed research on specific areas, as will be demonstrated in the next chapter of this thesis.

3. REGIONAL SALINITY CHARACTERIZATION AND DESALINATION EVALUATION: LOWER ARKANSAS RIVER VALLEY, COLORADO

3.1 Methodology

To achieve the second objective of this thesis, I studied a region identified as suitable through geospatial analysis to understand the water and salt balance along a major river and assess the effectiveness of applying desalination technologies to irrigation water, thereby improving the water quality of the river system. A segment of the Arkansas River in southeastern Colorado was selected as a case study (see Figure 9). Given the limited discrete salt ion measurements in the river, a Random Forest machine learning model was developed to generate synthetic salt ion concentration data for a 21-year study period (2000-2020), combined with a mass balance approach to illustrate the long-term salinity trends throughout the river system.

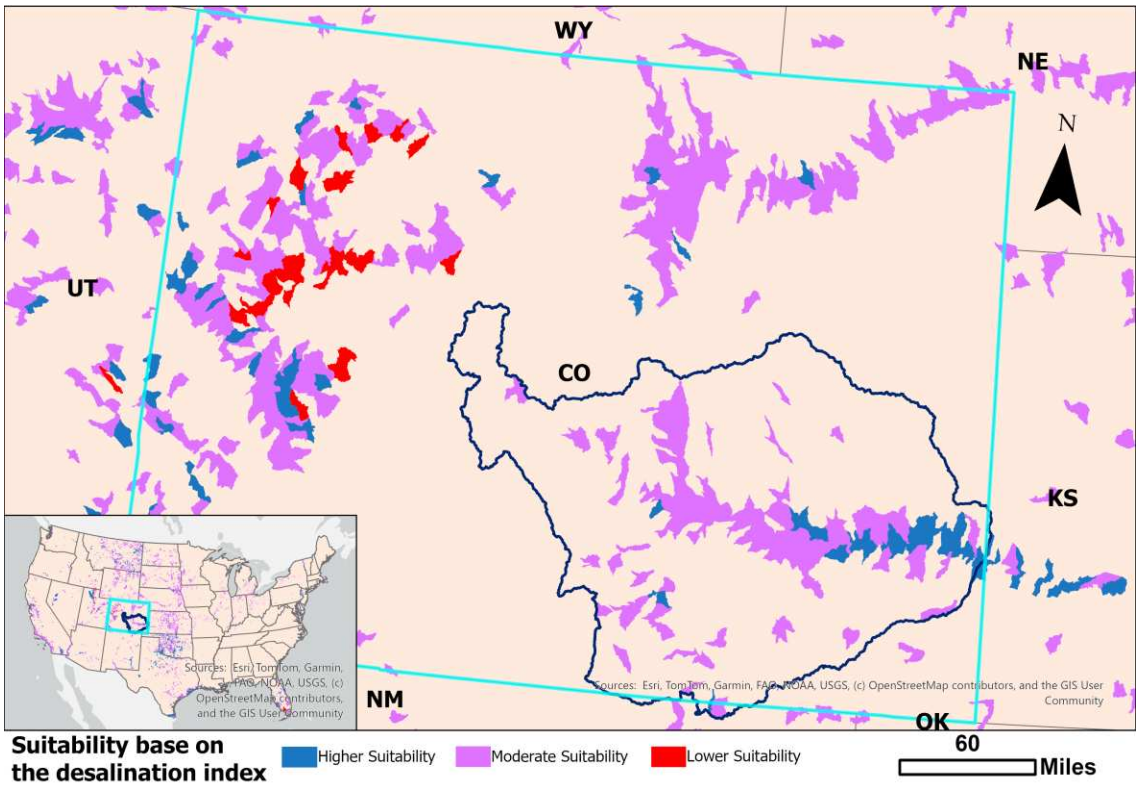

Figure 9: The study area chosen based on the results of the second chapter of this thesis, the Upper Arkansas watershed in Southeastern Colorado, includes the section of the Arkansas River designated for the case study.

Subsequently, a SWAT-MODFLOW-Salt model of a sub-region was used to evaluate the implementation of desalination on the river system, specifically the impact of on-farm desalination on groundwater salt loading to the Arkansas River.

3.1.1 Study Region

Based on Objective 1 (see Chapter 2), several HUC12 watersheds within the Lower Arkansas River Watershed in Colorado were identified as having moderate or higher suitability for agricultural desalination. This area has been irrigated since the 1870s, resulting in saline high water tables that began to develop in the early 20th century (Gates et al., 2002). This means the Lower Arkansas River Valley (LARV) is a typical expansive, long-irrigated stream-aquifer system affected by freshwater salinization (Morway & Gates, 2012). It has been considered as one of the more saline rivers of its size in the United States, leading to numerous studies in the

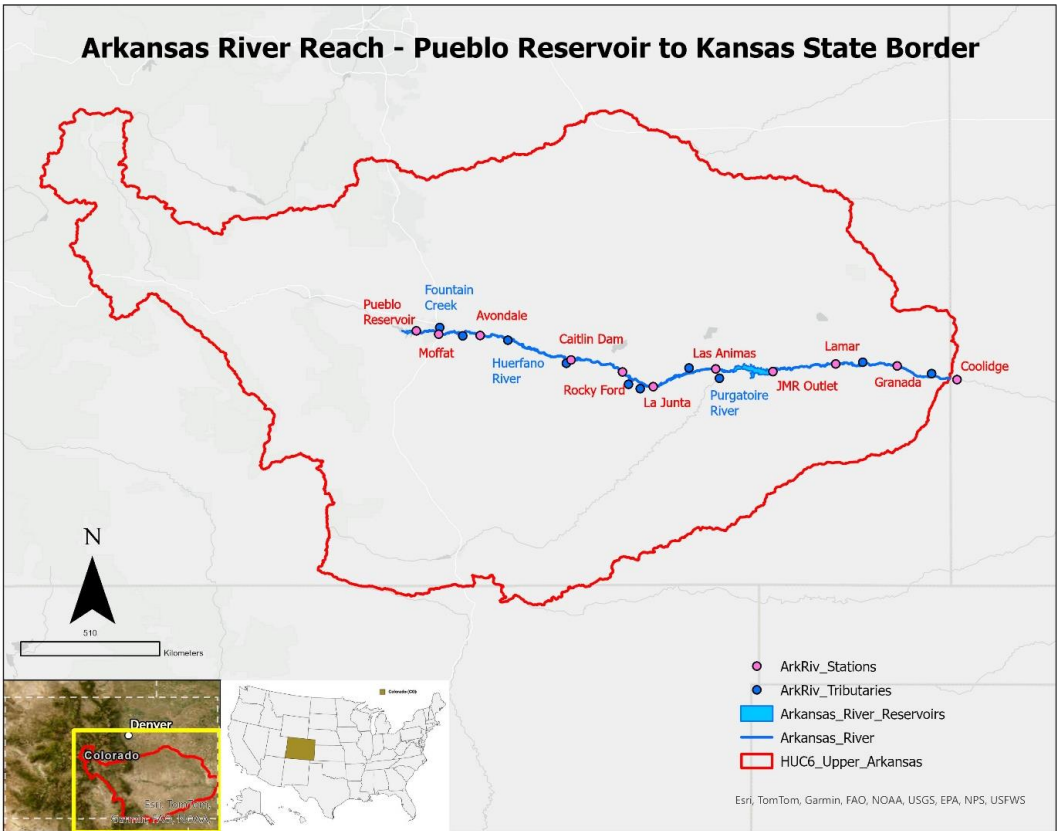

Figure 10: Map of the study region encompassing the segment of the Arkansas River analyzed in this study. This segment of the river is part of the wider Upper Arkansas HUC6 watershed highlighted in red.

literature that have focused on the water and salt dynamics of the river system. Therefore, a 317.5 km (197.3 mi) reach of the Arkansas River from the Pueblo Reservoir to the Coolidge station in the Colorado-Kansas state border was selected for further analysis, shown in Figure 10.

3.1.2 Salt Mass Balance in the Arkansas River

To characterize salt mass transport in the Arkansas River and the influence of on-farm desalination on groundwater salt loadings to the river, we applied a mass balance to sections of the Arkansas River between stream gaging stations. This approach requires estimating daily salt loadings at gaging sites along the river, in tributaries, and at locations of canal diversions (see Figure 10). Due to sparse salt ion concentration data at these locations, a machine learning approach was used to estimate daily in-stream concentrations, using datasets of measured daily streamflow discharge (DIS), measured daily specific conductance (SC), and measurements of discrete salt ion concentrations. This section provides details on locations of measurements. Section 3.1.3 provides details on the Random Forest model for estimating daily salt ion concentrations. Section 3.1.4 provides final details of the water balance and salt ion mass balance.

Historical measurements of salt ion concentrations, for six of the major salt ions (SO_4^{--}, Cl^-, Ca^{++}, Mg^{++}, Na^+, and K^+), discharge (DIS), and specific conductance (SC) were collected from multiple stations along the Arkansas River (see Figure 10). These variables were chosen for their widespread use as indicators of water salinity, as mentioned earlier. See Figure 11 for sample data from two gaging stations. The stations utilized are listed in Table 6, and the data were obtained from the USGS for salt ion concentrations and from the DWR for stream flow and specific conductance. These datasets were organized into Excel workbooks, with each sheet

representing a unique station. The data were cleaned and structured to ensure consistency in column naming and date formatting. For modeling purposes, salt ion concentrations (mg/L) served as the dependent variable, while SC (µS/cm) and DIS (m^3/s) acted as the independent variables.

Table 6: Gaging stations in the Arkansas River, whose data was used for training the machine learning models.

Station Name	DWR code	USGS code	Type
Arkansas River Above Pueblo	ARKPUECO	07099400	Main channel
Arkansas River at Moffat Street at Pueblo	ARKMOFCO	07099500*	Main channel
Fountain Creek at Pueblo	FOUPUECO	07106500	Tributary
Arkansas River Near Avondale	ARKAVOCO	07109500	Main channel
Arkansas River at Catlin Dam, Near Fowler	ARKCATCO	07119700	Main channel
Arkansas River Near Rocky Ford	ARKROCCO	07120500	Main channel
Arkansas River at La Junta	ARKLAJCO	07123000	Main channel
Arkansas River at Las Animas	ARKLASCO	07124000	Main channel
Purgatoire River Near Las Animas	PURLASCO	07128500	Tributary
Arkansas River Below John Martin Reservoir	ARKJMRCO	07130500	Main channel
Arkansas River at Lamar	ARKLAMCO	07133000	Main channel
Arkansas River Near Coolidge	ARKCOOKS	07137500	Main channel

*Discharge values were gathered from a station close by, the Arkansas River Near Pueblo, due to the incomplete time series of the station ARKMOFCO.

3.1.3 Machine Learning Model

Random Forest Regression (RFR), a machine learning ensemble method mentioned earlier, was chosen to predict salt ion concentrations based on SC and discharge values. The modeling was conducted individually for each station along the Arkansas River using Python's scikit-learn library (Pedregosa et al., 2011). The modeling workflow included the following steps: (1) data preparation, (2) initial model training, (3) hyperparameter tuning, (4) model evaluation, (5) uncertainty analysis, (6) visualization, and (7) model predictions.

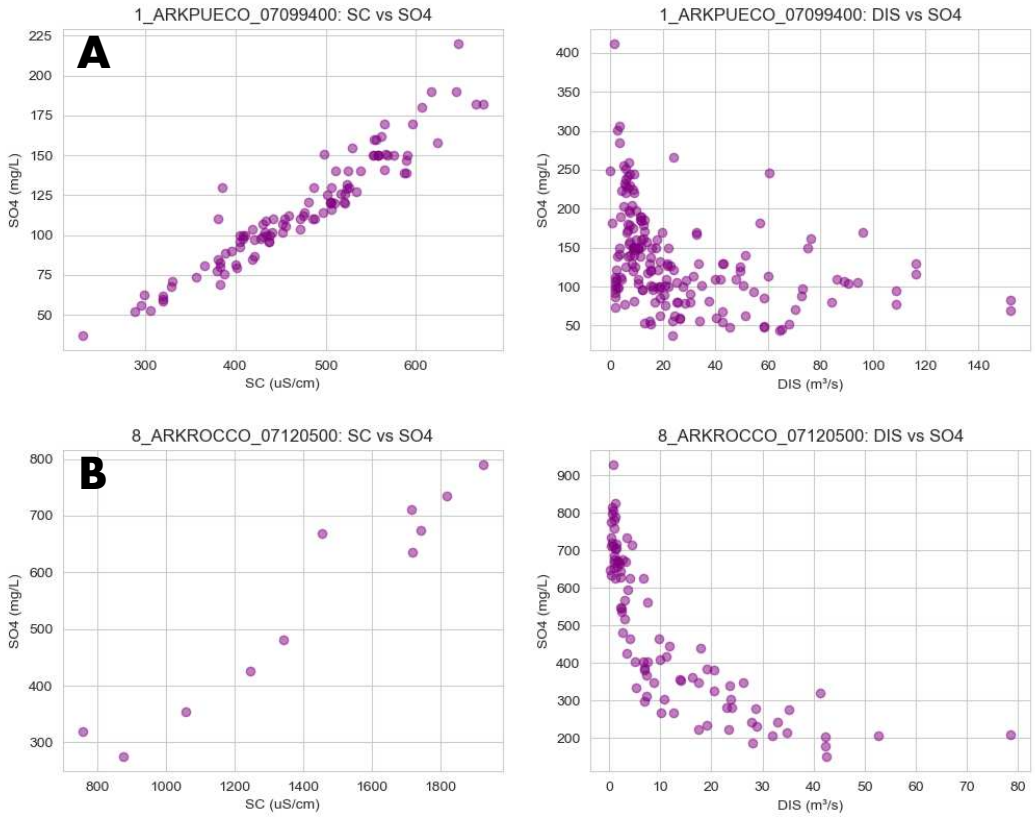

Figure 11: SO_4 machine learning model input data sample for the (A) ARKPUECO and (B) ARKROCCO stations.

First, three Excel files prepared in advance for each station are imported for data preparation. The three files contain the training data, input for future predictions, and model parameters. Subsequently, each station's dataset was randomly divided into training and testing sets using the test size specified in the model parameters file, typically 20%. A random state seed (123) was utilized to ensure reproducibility. Second, an initial Random Forest model was trained using default parameters to establish baseline performance metrics.

Third, hyperparameters were optimized using GridSearchCV to prevent overfitting and to identify the best combination of parameters for the model. A k-fold cross-validation (CV) method was also employed to more accurately measure the model's performance. The number of

folds, or subsets, is specified in the model parameters file. The parameters selected for model tuning include *n_estimators, max_depth, min_sample_split,* and *min_samples_leaf*. Constraining these parameters for regularization reduces the risk of overfitting by preventing the model from running indefinitely until it perfectly fits the training data (Géron, 2022). Similarly, the hyperparameter values for the hyperparameter grid input used in GridSearchCV are outlined in the model parameters file. The best-performing set of hyperparameters from the GridSearchCV method was trained on the entire training set and saved as the best-tuned model.

Fourth, the models were evaluated using standard statistical metrics, including the coefficient of determination (R^2), Mean Absolute Error (MAE), Root Mean Squared Error (RMSE), and the mean and standard deviation R^2 scores from cross-validation. Performance metrics were calculated and compared for both the initial and tuned models. Fifth, prediction uncertainty was assessed with an empirical method derived from the predictions of individual decision trees within the Random Forest ensemble. The prediction distribution from all trees was utilized to estimate salt ion concentrations, standard deviation (uncertainty), and empirical 95% confidence intervals (2.5th and 97.5th percentiles). Sixth, time-series plots were generated to interpret and validate model results. These visualizations illustrate the measured versus predicted salt ion concentrations, including empirical 95% confidence intervals. Discharge data were plotted in separate subplots to examine hydrologic influences on salt ion concentrations.

Seventh, each station's optimized Random Forest model was saved as a serialized Python object (pickle file) for future reuse and to ensure reproducibility. The models were applied to new datasets from the future predictions file uploaded earlier, which includes discharge and SC data for the 20-year study period. This was done to predict salt ion concentrations for the entire time series, calculate uncertainty and confidence intervals, and estimate salt ion loads using

Equation (2). Salt ion loads (kg/day) are estimated by multiplying the daily discharge (m^3/s) measured at the gaging station by the predicted salt ion concentration (mg/L) and a conversion factor of 86.4. The conversion factor standardizes units of volume (L to m^3), mass (mg to kg), and time (seconds to days). Finally, the results were exported to Excel spreadsheets along with the model's performance metrics.

$$Salt\ load\ \left(\frac{kg}{day}\right) = DIS\ \left(\frac{m^3}{s}\right) \times\ Salt\ ion\ concentration\ (\frac{mg}{L})\ \times\ 86.4 \qquad (2)$$

3.1.4 Mass Balance Analysis

To thoroughly evaluate salinity conditions in the river reach, a study period of 21 years was selected, spanning from 2000 to 2020. The synthetic data generated from the Random Forest models developed in the previous section is only available at each station location. Therefore, a simple mass balance approach was used to estimate discharge and salt ion loads spatially throughout the study reach. The study reach begins at the outlet of Pueblo Reservoir and follows the Arkansas River to the Coolidge station in Kansas. The reach was divided into 10 sections, each starting and ending with an instream station and potentially including one or several tributary or canal stations. from excessive irrigation, seepage from earthen canals, and inefficient drainage systems. Large

Table 7 lists the stations considered for each reach.

For each section, the input and output discharges are known from station discharge data, along with the inflow from the tributaries and outflow from the canal diversions, if present, in the section. A simple water balance approach was employed to determine unaccounted-for flows in each section (see Figure 12). These unaccounted flows were considered groundwater discharge

entering the river due to elevated water tables in the Lower Arkansas River Valley, resulting from excessive irrigation, seepage from earthen canals, and inefficient drainage systems. Large

Table 7: Sections of the study reach used for the mass balance calculations and their respective gauging stations.

Section	Station	DWR Code/Name or USGS Code	Station Type
Section 1	Pueblo Reservoir	ARKPUECO	Instream
	Moffat	ARKMOFCO	Instream
Section 2	Fountain Creek	FOUMOUCO	Tributary
	Excelsior	EXCELSIOR DITCH	Canal diversion
	St. Charles River	STCHARCO	Tributary
	Avondale	ARKAVOCO	Instream
Section 3	Colorado	COLORADO CANAL	Canal diversion
	Huerfano River	HUEBOOCO	Tributary
	Rocky Ford Highline	ROCKY FORD HIGHLINE	Canal diversion
	Oxford	OXFORD CANAL	Canal diversion
	Otero	OTERO CANAL	Canal diversion
	Apishapa River	APIFOWCO	Tributary
	Caitlin dam	ARKCATCO	Instream
Section 4	Caitlin	CATLIN CANAL	Canal diversion
	Holbrook	HOLBROOK CANAL	Canal diversion
	Rocky Ford Ditch	ROCKY FORD DITCH	Canal diversion
	Fort Lyon Storage	FORT LYON STORAGE CANAL	Canal diversion
	Rocky Ford	ARKROCCO	Instream
Section 5	Timpas Creek	TIMSWICO	Tributary
	Fort Lyon	FORT LYON CANAL	Canal diversion
	Crooked Arroyo	CANSWKCO	Tributary
	La Junta	ARKLAJCO	Instream
Section 6	Las Animas Consolidated	LAS ANIMAS CONSOLIDATED	Canal diversion
	Horse Creek	HRC194CO	Tributary
	Las Animas	USGS 07124000	Instream
Section 7	Purgatoire River	PURLASCO	Tributary
	John Martin Reservoir Outlet	ARKJMRCO	Instream
Section 8	Fort Bent	FORT BENT CANAL	Canal diversion
	Amity	AMITY CANAL	Canal diversion
	Lamar	LAMAR CANAL	Canal diversion
	Lamar	ARKLAMCO	Instream
Section 9	Hyde	HYDE DITCH	Canal diversion
	Big Sandy Creek	BIGLAMCO	Tributary
	Buffalo	BUFFALO CANAL (ARKANSAS)	Canal diversion

	Granada	ARKGRACO	Instream
Section 10	Wild Horse Creek	USGS 07134990	Tributary
	Frontier	FRODITKS	Canal diversion
	Coolidge	USGS 07137500	Instream

hydraulic gradients arise from the elevated water tables, which drive subsurface flow back to the main river channel (Morway & Gates, 2012). Equation (3) was used for the water balance of each section, where groundwater discharge or recharge (GW) is equal to the outlet station flow (O) minus the inflow station flow (I) minus the tributaries inflow (T) plus the canal diversions (C), with all units in m^3/s.

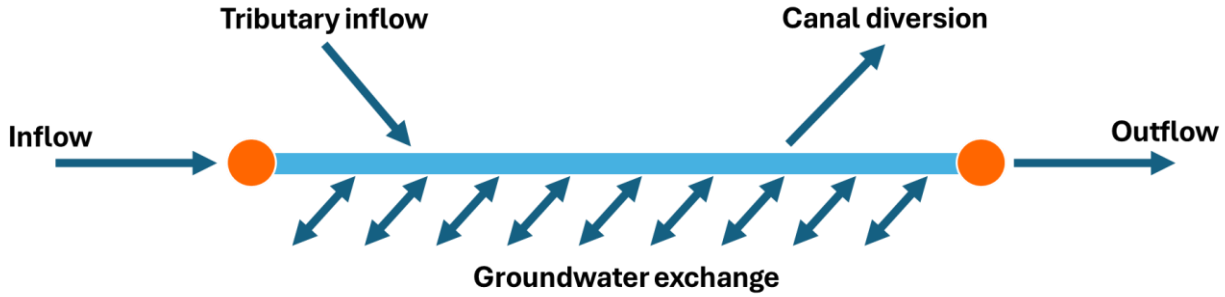

Figure 12: Diagram representing water and mass fluxes in a section of the river, between two gauging stations.

$$GW = O - I - T + C \quad (3)$$

Next, the water balance for each section was calculated daily throughout the entire time series, and the resulting groundwater exchange was averaged over the study period. The average groundwater exchange for each section was divided by the length of the river reach in that section, yielding the average flow per unit of distance (m^3/sec/km). Finally, the average flow of the entire study reach is plotted to visualize spatial gains and losses in the river along its length.

The same procedure described above was used to estimate daily salt ion loads (g/day) along the Arkansas River. Tributary loads are computed by multiplying measured daily tributary

inflows (m^3/day) by daily salt ion concentrations (g/m^3) provided by the Random Forest model. In-river loads are computed by multiplying measured daily river discharge by daily concentrations provided by the Random Forest model. Insufficient data was available for several stations considered in this analysis, particularly canal diversion locations. The average salt ion concentration of the nearest instream station was assigned to these stations, and the daily loads were calculated by multiplying the assigned concentration by the daily discharge. Subsequently, the average load per unit of distance (kg/day/km) was calculated and plotted to illustrate salt loads throughout the study reach.

3.1.5 SWAT-MODFLOW-Salt Model

The increasing significance of desalination technologies has been previously emphasized, and this study aims to evaluate their implementation in the study region to improve stream water quality. Consequently, a SWAT-MODFLOW-Salt model, developed by (Bailey & Hosseini, 2023) and applied to a 700 km² irrigated section of the Lower Arkansas River Valley, this model was utilized to evaluate the application of desalination technologies in the study area. The model covers a ten-year period, from 2001 to 2010, and includes three gaging stations along the river (Rocky Ford, La Junta, and Las Animas) as well as two tributary gaging stations (Crooked Arroyo and Timpas Creek).

SWAT-MODFLOW-Salt is an integrated hydrologic and salinity transport modeling tool that combines the Soil and Water Assessment Tool (SWAT), MODFLOW, and RT3D codes into a single executable for model simulation. SWAT simulates land surface, soil, and stream hydrologic processes, while MODFLOW models groundwater-surface water exchange and other groundwater hydrologic processes. Additionally, the groundwater reactive transport code RT3D simulates the fate and transport of nutrients. The model code is further modified to include the

transport and fate of the eight major salt ions (SO_4^{2-}, Cl^-, CO_3^{2-}, HCO_3, Ca^{2+}, Na^+, Mg^{2+}, K^+) to create SWAT-MODFLOW-Salt. This model accounts for interactions among surface water, soil moisture, and groundwater, including groundwater-surface water exchanges, groundwater recharge, irrigation practices, and the reactions involving the dissolution and precipitation of salt minerals.

The effectiveness of desalination was evaluated by comparing modeled groundwater loads discharged into the river under scenarios with and without desalination interventions. The SWAT-MODFLOW-Salt model was first run using the default scenario with no desalination applied. Next, a scenario was executed in which desalination was applied to eliminate 50% of the salt ion mass in the irrigated hydrologic response units (HRUs). These HRUs were selected by intersecting the HRU layer with the irrigated lands feature class layer used in Chapter 2 of this thesis for the geospatial analysis. The percentage reduction in salt ion loads from both scenarios was calculated by dividing the total loads over the simulation period. This percentage reduction is applied to the average salt ion loads calculated in the previous section.

3.2 Results

Each of the Random Forest models trained for the stations in the study area was used to generate a time series of salt ion concentrations for the study period for each of the salt ions considered in this study (SO_4^-, Cl^-, Ca^{++}, Mg^{++}, Na^+, and K^+). Two examples of these time series for SO_4 concentrations are shown in Figure 13. SO_4 was chosen because it is the predominant salt ion in the river, making up an average of 62% of the total salt loads. All remaining time series graphs from the stations are included in the supplemental materials of this thesis. It can be observed that measured values fall within the model prediction confidence interval, and the predictions capture the general trend of these values. The general pattern,

however, indicates that SO_4 concentrations reach a dynamic equilibrium and primarily fluctuate seasonally. Nevertheless, periods of drought directly increase sulfate concentrations over time, as seen in Figure 13A. During the dry years of 2002 and 2003, a significant increase in SO_4 concentrations was noted at the Pueblo Reservoir station. The opposite effect occurs during increased streamflow events, which typically result in a rapid decrease in SO_4 concentrations. A clear example can be seen in the data from the Rocky Ford gaging station for 2017, as shown in Figure 13B.

Furthermore, Table 8 presents the statistical parameters for each station, which are used to evaluate the SO_4 model's performance. Overall, the models' performances are acceptable, with good results for the coefficient of determination, MAE, and RMSE. However, performance declines at the latter stations, despite most having a good number of training samples. Generally, lower discharge values were observed at these stations, along with highly variable SO_4 concentrations and fewer specific conductance measurements available, indicating that the algorithm has more difficulty modeling SO_4 concentrations at these locations.

Table 8: Machine Learning SO_4 models' performance metrics for each gauging station.

Station	Tuned R^2	CV mean R^2	MAE (mg/L)	RMSE (mg/L)
ARKPUECO	0.79	0.64	16.15	22.43
ARKMOFCO	0.77	0.73	87.88	149.10
FOUPUECO	0.80	0.64	35.36	49.36
ARKAVOCO	0.79	0.84	23.62	34.51
ARKCATCO	0.79	0.91	42.19	64.61
ARKROCCO	0.91	0.79	54.41	62.95
ARKLAJCO	0.86	0.58	100.45	112.24
ARKLASCO	0.40	0.67	276.15	366.32
PURLASCO	0.46	0.60	427.46	499.64
ARKJMRCO	0.69	0.63	272.20	363.92
ARKLAMCO	0.58	0.36	347.40	405.46
ARKCOOKS	0.46	0.63	293.28	377.80

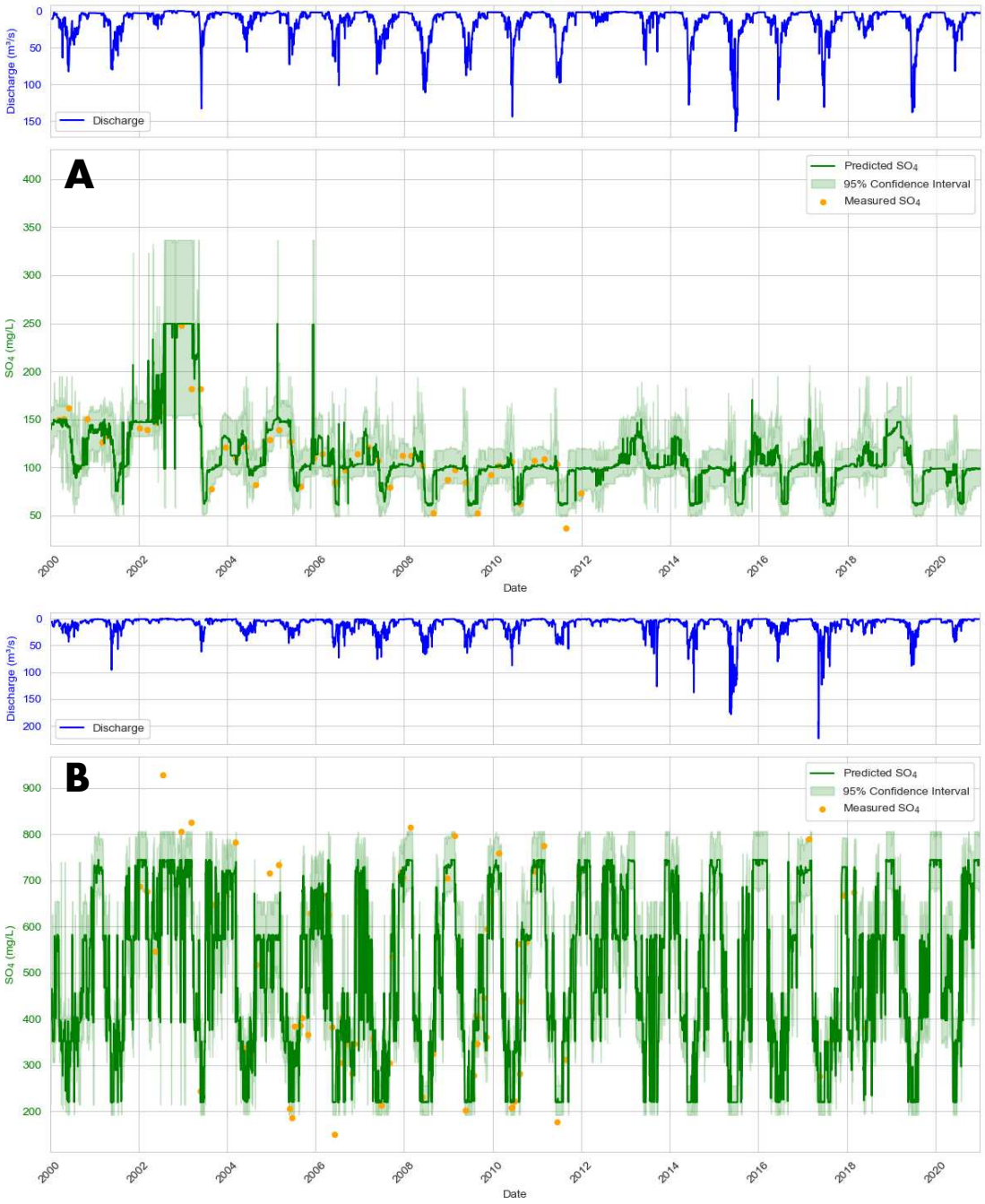

Figure 13: Time series of synthetic data of sulfate concentrations, generated by the Random Forest Model, in green, instream discharge measurements from its respective gaging station, in blue, and sulfate concentration measurements in yellow. Two stations are shown, the (A) Arkansas River Above Pueblo gauging station at the top, and the (B) Arkansas River Near Rocky Ford at the bottom.

Another notable difference is the significant disparity between the tuned R^2 and CV mean R^2 values at certain stations. The tuned R^2 corresponds to the model trained with the best performing set of parameters; on the other hand, the CV mean R^2 is calculated from the mean R^2 of all models tried during the cross-validation process used as part of the model training. As mentioned previously, cross-validation is a valuable tool for determining the optimal parameters of the model. However, it can also serve as an indicator of the model's robustness and ability to generalize. A good CV mean R^2 value may suggest strong performance across different data sets. Additionally, when paired with a relatively similar tuned R^2 value, it indicates that the model is performing as expected. The ARKMOFCO and ARKJMRCO stations, as shown in Table 8, exhibit this behavior. Furthermore, when a good CV mean R^2 is paired with an even higher tuned R^2, it indicates that the model is outperforming its expected performance. Performance metrics from the ARKPUECO and ARKROCCO stations illustrate this scenario. Conversely, if the tuned R^2 value is lower than the CV mean R^2, it may indicate that the model is overfitting the training data and generalizing poorly when tested against unseen data. The ARKVOCO and ARKCATCO stations are good examples of this scenario.

Average flow and SO_4 loads throughout the Arkansas River, according to the mass balance analysis, are depicted in Figure 14 and Figure 16, respectively. Average flow is exhibiting a downward trend as it moves away from the Pueblo Reservoir. This is mainly due to the significant amount of water being diverted to canals for irrigation, as indicated in Table 9. However, the average canal diversion discharge exceeds the combined average reservoir inflow and tributary inflow into the river, which could render it unsustainable if not for the considerable groundwater discharge returning to the river. Groundwater discharge is evident in the sloped sections of the average flow graph in Figure 14.

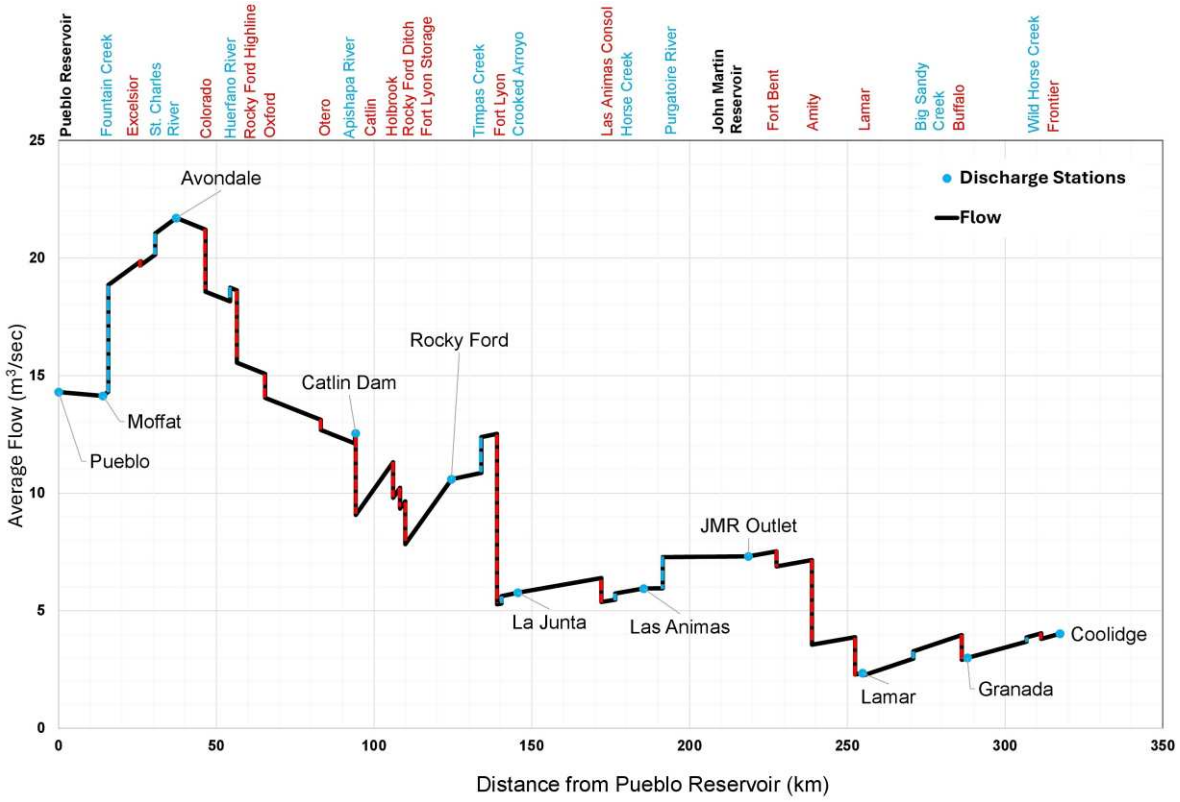

Figure 14: Spatial variation of average flow (m^3/s) in the Arkansas River study reach for the 21-year study period (2000-2020).

In contrast to average flows, SO_4 loads (see Figure 15) exhibit an upward trend downstream due to groundwater discharge, which controls SO_4 loading in the river system. Approximately 65.6% of the SO_4 loads entering the river come from groundwater discharge, as illustrated in the pie chart from Figure 17. Consequently, Figure 15 shows that SO_4 concentrations are increasing downstream due to the decreasing river flow, combined with the rising loads mentioned earlier. Additionally, a significant amount of sulfate is being diverted through canals into the irrigation water canals (see Table 9).

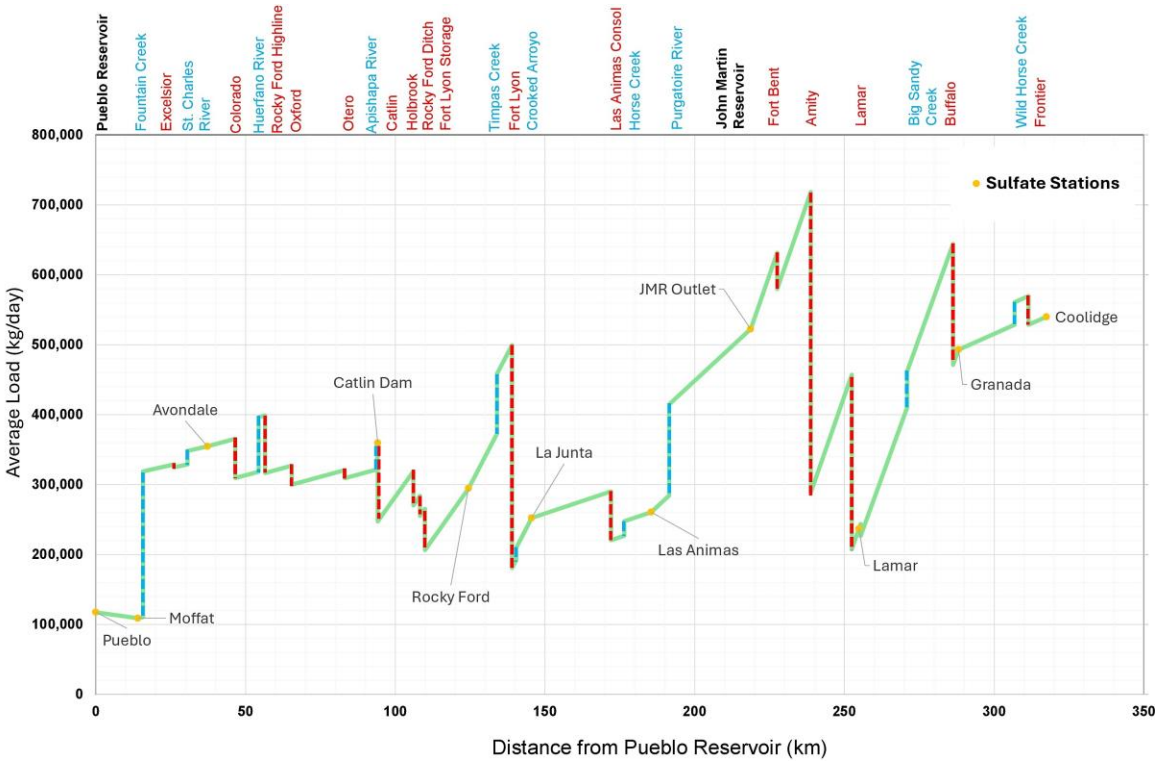

Figure 16: Spatial variation of SO_4 loads (kg/day) in the Arkansas River.

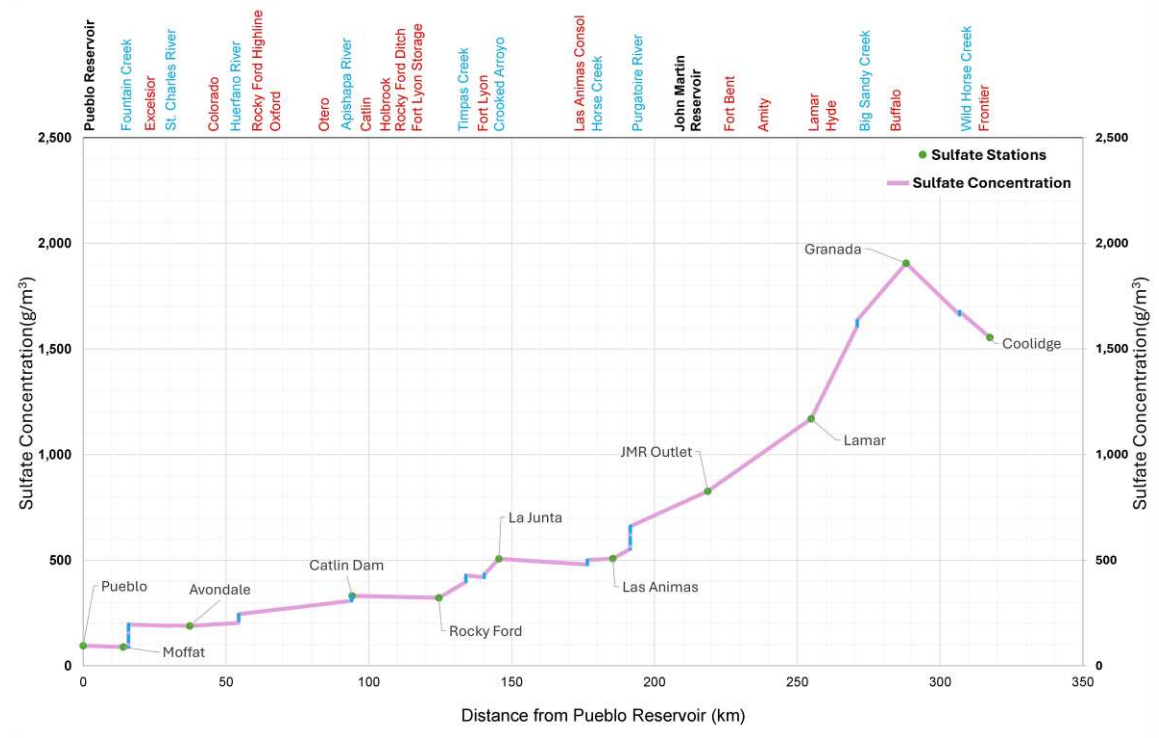

Figure 15: Spatial variation of average sulfate concentrations in the Arkansas River.

Table 9: Average results of discharge and SO_4 loads in the Arkansas River study reach, from the Pueblo Reservoir to the Coolidge gaging station.

Source	Discharge (m^3/s)	SO_4 Load (kg/day)
Reservoir inflow	14.3	117,474.9
Total tributary inflow	10.4	681,142.8
Total canal diversions	30.5	1,780,236.6
Total outflow	4.0	539,916.8
Groundwater inflow	9.9	1,521,535.6

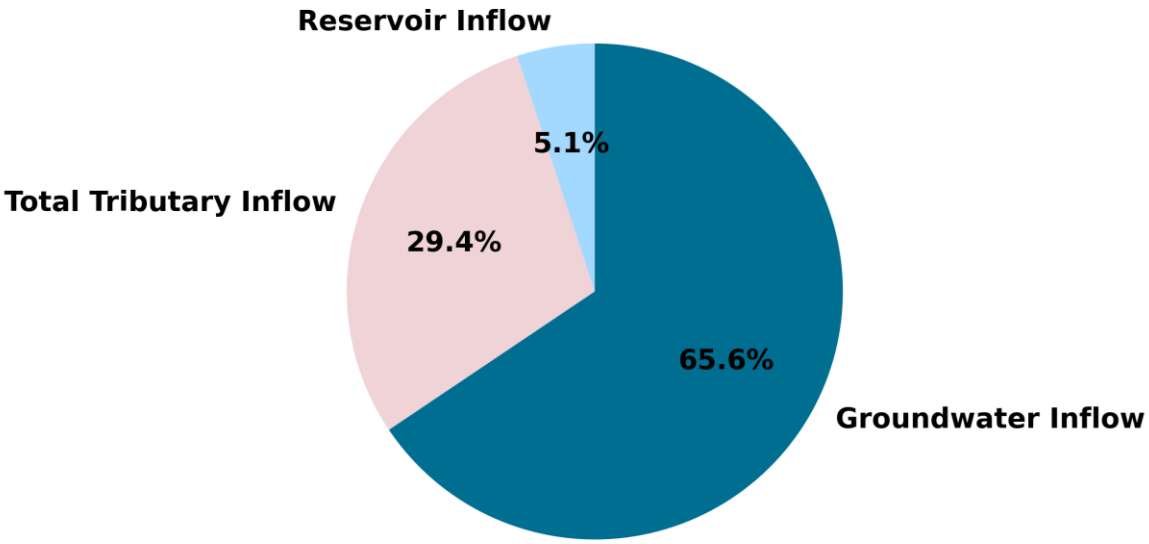

Figure 17: Pie chart of the distribution of SO_4 loads into the river from different sources.

Similar results were observed for most of the salt ions considered in this study (Cl^{-}, Ca^{++}, Mg^{++}, Na^{+}, and K^{+}). Nevertheless, SO_4 emerged as the dominant salt ion, exhibiting the most significant average loading in the study region, see Figure 18. Additionally, K concentrations were notably lower than those of the other salt ions. Consequently, the Random Forest algorithm was unable to generate a model for any station below Avondale, as indicated in Figure 18, where K loads cease. Furthermore, groundwater accounts for the majority of total salt ion loads entering the river (see Figure 19), comprising 68.7% of total inflows, which aligns with the observed SO_4 results. Likewise, similar findings were noted for canal diversions, where a substantial amount of total salt ion loads (2,823,950 kg/day) is diverted through canals into the irrigation water, see Table 10.

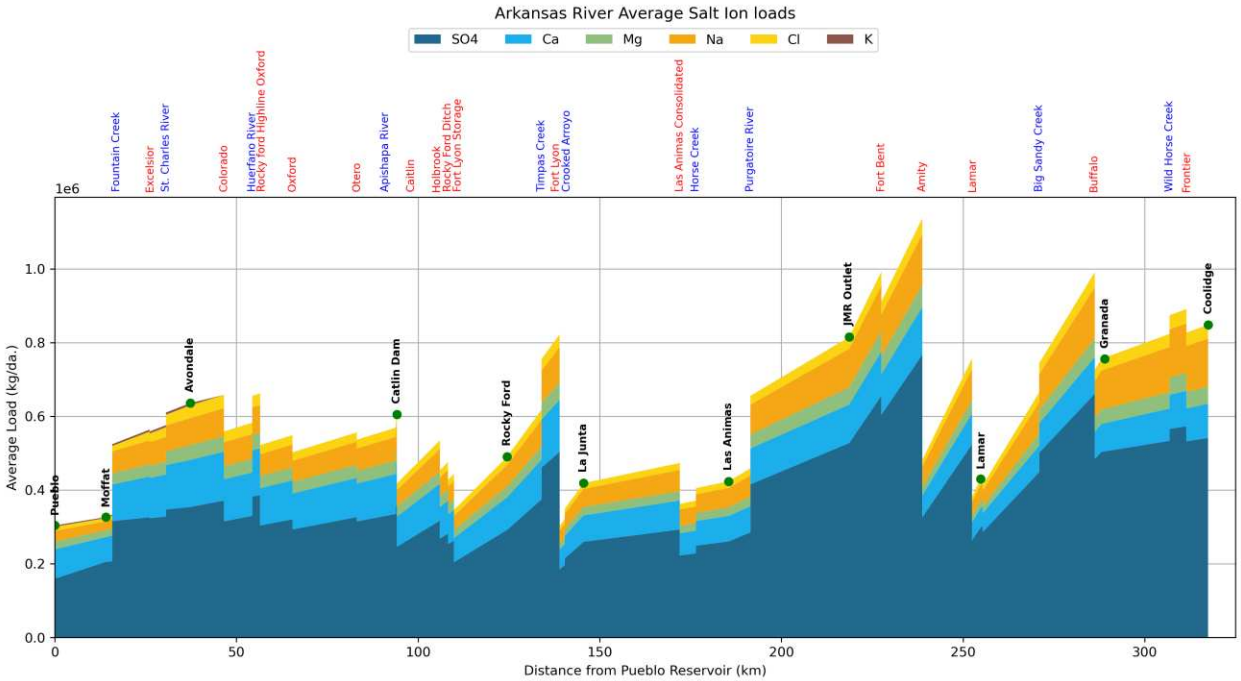

Figure 18: Average area load graph for discrete salt ions in the Arkansas River in kg/day.

Table 10: Average results of discharge and total salt ion loads in the Arkansas River

Source	Discharge (m^3/s)	Total loads (kg/day)
Reservoir inflow	14.3	304,049
Total tributary inflow	10.4	862,122
Total canal diversions	30.5	2,823,950
Total outflow	4.0	906,991
Groundwater inflow	9.9	2,564,770

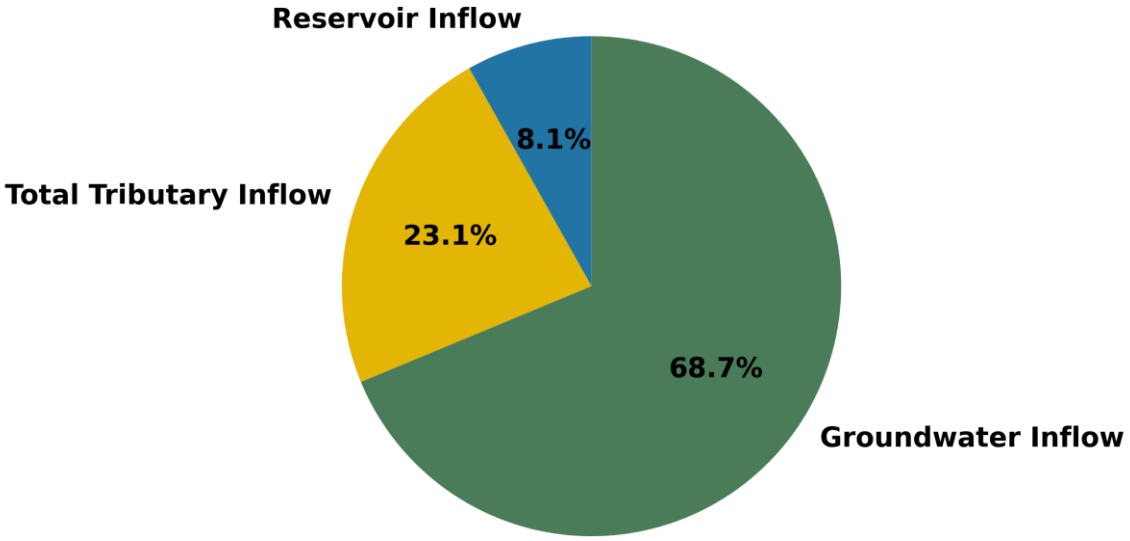

Figure 19: Pie chart of the distribution of total salt ion loads into the river from different sources.

Desalination was proposed as a solution to high salt ion concentrations in the river system, aiming to improve irrigation water quality and reduce the salt ion load discharged into the groundwater from the river. Results for the two scenarios run in the SWAT-MODFLOW-Salt model are shown in Figure 20. A baseline scenario with no desalination and a scenario with 50% desalination of the applied irrigation water were used. Both scenarios exhibited very similar results regarding annual sulfate loads from groundwater into the river, with the latter years stabilizing and plateauing after the initial warm-up period, a result of the model's initial conditions. However, there is no noticeable improvement in groundwater discharge despite the application of desalination to HRUs with irrigated fields. These average yearly loads remain

almost unchanged for both scenarios during the study period, as shown in Table 11, indicating that river salinity conditions are unlikely to change for the scenario with 50% desalination.

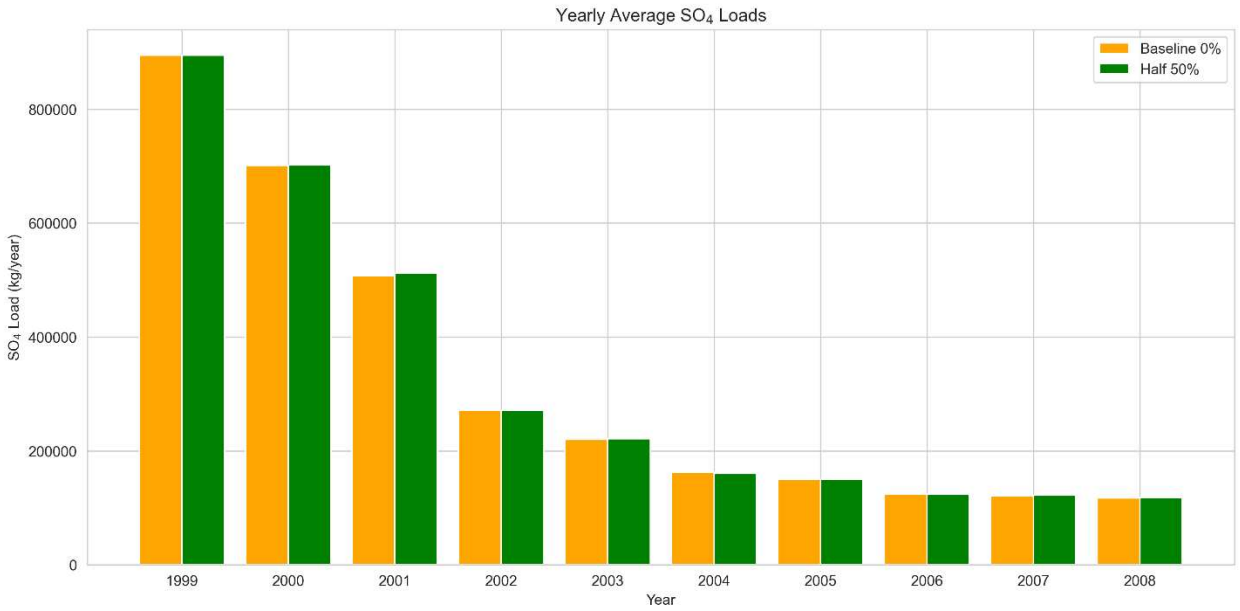

Figure 20: Yearly average sulfate loads into the river. Results are shown from the SWAT-MODFLOW-Salt model for the two scenarios considered.

Table 11: Yearly average sulfate loads into the river from the SWAT-MODFLOW-Salt model.

	Yearly Sulfate Loads from Groundwater into Surface Water ($1x10^5$ kg/yr.)									
Scenario	1999	2000	2001	2002	2003	2004	2005	2006	2007	2008
Baseline (0%)	8.95	7.01	5.08	2.71	2.20	1.63	1.50	1.24	1.21	1.17
Half (50%)	8.95	7.02	5.12	2.71	2.21	1.60	1.50	1.24	1.22	1.18

3.3 Discussion

Groundwater discharge and salinity loads into the Arkansas River from return flows resulting from over-irrigation have been well-documented in the literature (Gates et al., 2002; Goff et al., 1998; Lin & Garcia, 2012; Morway & Gates, 2012; Osborn, 2019). Results from this study are consistent with these findings; for instance, 29% of the water inflow estimated into the river is attributed to groundwater discharge. Furthermore, 68.7% of the salt ion loads estimated

are introduced into the river system via groundwater. Similarly, a study by (Cain, 1985) on a small irrigated area in the Lower Arkansas Valley over a two-year period reported that 88% of the applied salt in irrigation water was returned to the river system through groundwater. As a result, several studies have aimed to address the irrigation-induced salinization in one of the most affected regions in the United States (Gates et al., 2002).

In this study, we aimed to utilize emerging technologies in desalination to enhance water quality in the river system. Desalination technologies have seen wider adoption and decreased costs in recent years (Musie & Gonfa, 2023). However, results over a 10-year period did not show any significant reductions in sulfate loads entering the river, indicating there will likely be no changes to the river's salt balance and, consequently, the stream water quality. This could be explained by the relatively slow movement of subsurface flow, perhaps because the irrigation water applied takes too long to return to the main channel, thus the 10-year period of the simulation was not enough. Furthermore, another explanation could be that irrigation water is not the main source of salt solutes; instead, the dissolution of salt ions from the alluvial aquifer might be the primary source of salt.

Other studies have explored different approaches to target the issue, with varied results. For instance, (Goff et al., 1998) applied a scenario in which irrigation from both groundwater and surface water sources was stopped, seeing average monthly river salinity decrease by 4.4%. However, after 12 years, the system reached a new dynamic equilibrium. A similar approach was taken by (Lin & Garcia, 2012) by stopping the irrigation service for the areas supplied by three major canals. The aim is to alter the water and salt balance in the river to reduce groundwater return flows that carry salt loads into the river. Three scenarios were tested, yielding varying

results, ranging from a 5.3% decrease in river salinity to a 6.3% increase, and a scenario with an insignificant change in river salinity.

It is worth mentioning the large time scales at which salinity has affected the region; the study area has been under irrigation since the 1870s (Morway & Gates, 2012). Thus, the 10-year period used in the desalination scenario may not be sufficient, and more years or decades may be necessary to alter the salt balance of the river using this approach alone. The other studies referenced took a different approach by reducing irrigation water consumption levels to varying degrees. Nevertheless, as previously emphasized in this thesis, a rising global population is leading to an increasing demand for irrigated agriculture; therefore, attempting to reduce the water sources for irrigated agriculture may not be the most appropriate solution.

Perhaps a more holistic approach in future studies to tackling the issue of irrigated-induced salinity could yield better results. The long-term goal of altering the river salt balance should be targeted through management strategies, primarily the reduction of salt loads into the river. However, these management strategies require the involvement of all stakeholders, including irrigators and canal operators. Hence, management strategies that target short-term gains, such as increased crop yields and improved soil salinity, must also be considered. Desalination of irrigation water has proven to increase crop yields and would reduce the amount of nutrients reaching the ground. The amount of soluble salt in precipitation water, combined with the volume of water applied, determines the amount of salt added to the soil from irrigation water (Ghassemi et al., 1995). Hence, desalination can be a valuable tool for reducing salt concentrations in water and, consequently, mitigating soil salinization. This could be paired with other management practices that have already been suggested for the region in the Lower Arkansas River Watershed (LARW) management plan (Osborn, 2019). Instead of curtailing

irrigation water, more efficient irrigation techniques, such as sprinklers or drip irrigation, should be adopted to replace the inefficient flood irrigation methods commonly employed in the region. Additionally, canal lining or sealing will reduce groundwater flows by preventing recharge to the aquifer. Consequently, over time, changes to the water and salt balance should be observed. The LARW management plan also suggests other best management practices to consider, including fallowing, nutrient management planning, improved riparian buffers, conservation tillage, irrigation scheduling, and soil moisture monitoring.

Finally, more comprehensive tools should be utilized to test these management scenarios over adequate time frames to ascertain whether meaningful results are achieved in a reasonable timeframe.

4. CONCLUSIONS

This thesis aimed to identify suitable sites for agricultural desalination in the contiguous United States, to mitigate the environmental and economic impacts of freshwater salinization. HUC12 watersheds were characterized using GIS datasets and further assessed for their suitability for desalination technologies powered by renewable energy. However, due to the complexity of river systems and the importance of long-term salinity monitoring and assessment, a more detailed study for suitable regions was considered. As a result, we aimed to delve deeper into one of the previously identified regions to gain a better understanding of water and salt dynamics, as well as the effects of applying desalination as a management strategy to improve the water quality of the river system. A machine learning model was employed to generate synthetic data for a 21-year study period (2000-2020) and was used in conjunction with a mass balance approach to characterize water and salt fluxes throughout the Arkansas River spatially. Finally, a SWAT-MODFLOW-Salt model was used to test desalination as a management strategy.

Several regions in the CONUS have many watersheds deemed suitable for agricultural desalination technologies, especially in the water-stressed American West. Both surface water and groundwater sources were evaluated, revealing that areas in the Rocky Mountains, the Southwest, and the Plains regions showcase a significant number of HUC12 watersheds identified as suitable for agricultural desalination. The Great Lakes region, along with California in the Far West and Florida in the Southeast, also displayed a smaller but notable number of suitable watersheds. Altogether, there is a massive potential for the application of these emerging technologies and a need to address freshwater salinization issues nationwide. Nonetheless, this analysis is not a comprehensive examination of these sites; therefore, these results should be

considered a preliminary step toward a more detailed analysis of each specific region. Furthermore, factors such as economic and regulatory feasibility, government incentives, and the willingness to adopt these technologies should be considered in future studies to enhance this tool and achieve more robust results.

Groundwater discharge into the Arkansas River was found to be essential for maintaining the large amounts of water diverted through canals for irrigation purposes, accounting for 29% of the water inflow into the river system. However, this groundwater discharge mainly results from irrigation water return fluxes, which carry salt ions in the aquifer to the river system. Sulfate, the predominant salt ion in the water, was found to come primarily from groundwater discharge, representing 65.6% of the total sulfate inflows. Additionally, desalination was tested as a management practice over a 10-year period to enhance water quality in the river system. However, the results indicated that the river's salinity levels were unlikely to change. Despite this, the results from this study provide insight into the salinity issue that has plagued the Arkansas River for decades, offering a platform for evaluating further management strategies aimed at improving water quality in the river system. At the same time, a reduction in performance from the machine learning models downstream indicates that there is room for improvement and the potential to present more accurate results. Moreover, the limited number of gauging stations available poses a challenge to spatially characterizing salinity in the river system, leading to the reliance on assumptions for reaches with no measurement data to inform model building. Furthermore, this case study sets a good precedent for heavily irrigated semi-arid regions; however, caution must be exercised regarding generalization due to the myriad climate and geographic differences among all the sites identified nationwide. Future work should focus on improving the model for generating synthetic data by collecting and incorporating more

data. A different modeling approach can be explored by treating the entire river system as a single model, introducing spatial and temporal variables. A more holistic approach could be adopted to incorporate both short-term and long-term improvements, and this should be tested using more robust tools that encompass a larger area and a broader time frame.

By strategically identifying where desalination can support agriculture and mitigate the impacts of salinity on river systems, this research provides a decision-support foundation for managing agricultural water salinity, leveraging GIS, artificial intelligence, and modeling tools.

5. REFERENCES

Abu El-Maaty, A. E., Awad, M. M., Sultan, G. I., & Hamed, A. M. (2023). Innovative Approaches to Solar Desalination: A Comprehensive Review of Recent Research. *Energies*, *16*(9), Article 9. https://doi.org/10.3390/en16093957

Ali Khan, M., Izhar Shah, M., Faisal Javed, M., Ijaz Khan, M., Rasheed, S., El-Shorbagy, M. A., Roshdy El-Zahar, E., & Malik, M. Y. (2022). Application of random forest for modelling of surface water salinity. *Ain Shams Engineering Journal*, *13*(4), 101635. https://doi.org/10.1016/j.asej.2021.11.004

Alnahit, A. O., Mishra, A. K., & Khan, A. A. (2022). Stream water quality prediction using boosted regression tree and random forest models. *Stochastic Environmental Research and Risk Assessment*, *36*(9), 2661–2680. https://doi.org/10.1007/s00477-021-02152-4

Amer, R. (2021). Spatial Relationship between Irrigation Water Salinity, Waterlogging, and Cropland Degradation in the Arid and Semi-Arid Environments. *Remote Sensing*, *13*(6), Article 6. https://doi.org/10.3390/rs13061047

Androwski, J., Springer, A., Acker, T., & Manone, M. (2011). Wind-Powered Desalination: An Estimate of Saline Groundwater in the United States. *JAWRA Journal of the American Water Resources Association*, *47*(1), 93–102. https://doi.org/10.1111/j.1752-1688.2010.00493.x

Angelakis, A. N., Valipour, M., Choo, K.-H., Ahmed, A. T., Baba, A., Kumar, R., Toor, G. S., & Wang, Z. (2021). Desalination: From Ancient to Present and Future. *Water*, *13*(16), Article 16. https://doi.org/10.3390/w13162222

Ayers, R. S., & Westcot, D. W. (with Food and Agriculture Organization of the United Nations). (1985). *Water quality for agriculture*. Food and Agriculture Organization of the United Nations.

Bailey, R. T., & Hosseini, P. (2023). Comprehensive simulation of salinity transport in irrigated watersheds using an updated version of SWAT-MODFLOW. *Environmental Modelling & Software*, *159*, 105566. https://doi.org/10.1016/j.envsoft.2022.105566

Barron, O., Ali, R., Hodgson, G., Smith, D., Qureshi, E., McFarlane, D., Campos, E., & Zarzo, D. (2015). Feasibility assessment of desalination application in Australian traditional agriculture. *Desalination*, *364*, 33–45. https://doi.org/10.1016/j.desal.2014.07.024

Behrouz, M. S., Yazdi, M. N., & Sample, D. J. (2022). Using Random Forest, a machine learning approach to predict nitrogen, phosphorus, and sediment event mean concentrations in urban runoff. *Journal of Environmental Management*, *317*, 115412. https://doi.org/10.1016/j.jenvman.2022.115412

Ben-Gal, A., Yermiyahu, U., & Cohen, S. (2009). Fertilization and Blending Alternatives for Irrigation with Desalinated Water. *Journal of Environmental Quality*, *38*(2), 529–536. https://doi.org/10.2134/jeq2008.0199

Boryan, C., Yang, Z., Mueller, R., & Craig, M. (2011). Monitoring US agriculture: The US Department of Agriculture, National Agricultural Statistics Service, Cropland Data Layer Program. *Geocarto International*, *26*(5), 341–358. https://doi.org/10.1080/10106049.2011.562309

Breiman, L. (1996). Bagging predictors. *Machine Learning*, *24*(2), 123–140. https://doi.org/10.1007/BF00058655

Burn, S., Hoang, M., Zarzo, D., Olewniak, F., Campos, E., Bolto, B., & Barron, O. (2015). Desalination techniques—A review of the opportunities for desalination in agriculture. *Desalination*, *364*, 2–16. https://doi.org/10.1016/j.desal.2015.01.041

Cain, D. (1985). *Quality of the Arkansas River and Irrigation-return Flows in the Lower Arkansas River Valley, Colorado*. U.S. Department of the Interior, Geological Survey.

Cunillera-Montcusí, D., Beklioğlu, M., Cañedo-Argüelles, M., Jeppesen, E., Ptacnik, R., Amorim, C. A., Arnott, S. E., Berger, S. A., Brucet, S., Dugan, H. A., Gerhard, M., Horváth, Z., Langenheder, S., Nejstgaard, J. C., Reinikainen, M., Striebel, M., Urrutia-Cordero, P., Vad, C. F., Zadereev, E., & Matias, M. (2022). Freshwater salinisation: A research agenda for a saltier world. *Trends in Ecology & Evolution*, *37*(5), 440–453. https://doi.org/10.1016/j.tree.2021.12.005

Custodio, E. (2002). Aquifer overexploitation: What does it mean? *Hydrogeology Journal*, *10*(2), 254–277. https://doi.org/10.1007/s10040-002-0188-6

Davis, N. N., Badger, J., Hahmann, A. N., Hansen, B. O., Mortensen, N. G., Kelly, M., Larsén, X. G., Olsen, B. T., Floors, R., Lizcano, G., Casso, P., Lacave, O., Bosch, A., Bauwens, I., Knight, O. J., Loon, A. P. van, Fox, R., Parvanyan, T., Hansen, S. B. K., … Drummond, R. (2023). *The Global Wind Atlas: A High-Resolution Dataset of Climatologies and Associated Web-Based Application*. https://doi.org/10.1175/BAMS-D-21-0075.1

Donald Martin, Robert S Regan, Jonathan V Haynes, Amy L Read, Wesley Henson, Jana S Stewart, Justin Brandt, & Richard Niswonger. (2024). *Irrigation water use reanalysis for the 2000-20 period by HUC12, month, and year for the conterminous United States (ver.*

2.0, September 2024) [Dataset]. U.S. Geological Survey. https://doi.org/10.5066/P9YWR0OJ

Eldeiry, A., & Garcia, L. (2004). *Spatial Modeling using Remote Sensing, GIS, and Field Data to Assess Crop Yield and Soil Salinity*.

Galvani, A. (2007). The challenge of the food sufficiency through salt tolerant crops. In R. Amils, C. Ellis-Evans, & H. Hinghofer-Szalkay (Eds.), *Life in Extreme Environments* (pp. 437–450). Springer Netherlands. https://doi.org/10.1007/978-1-4020-6285-8_28

Garcia, L. A., Foged, N., & Cardon, G. E. (2006). Development of GIS-Based Model to Estimate Relative Reductions in Crop Yield due to Salinity and Waterlogging. *Journal of Irrigation and Drainage Engineering*, *132*(6), 553–563. https://doi.org/10.1061/(ASCE)0733-9437(2006)132:6(553)

Gates, T. K., Burkhalter, J. P., Labadie, J. W., Valliant, J. C., & Broner, I. (2002). Monitoring and Modeling Flow and Salt Transport in a Salinity-Threatened Irrigated Valley. *Journal of Irrigation and Drainage Engineering*, *128*(2), 87–99. https://doi.org/10.1061/(ASCE)0733-9437(2002)128:2(87)

Gelburd, D. E. (n.d.). *Managing salinity Lessons from the past*.

Géron, A. (2022). *Hands-On Machine Learning with Scikit-Learn, Keras, and TensorFlow, 3rd Edition* (Third Edition). O'Reilly Media, Inc. https://learning.oreilly.com/library/view/hands-on-machine-learning/9781098125967/

Ghassemi, F., Jakeman, A. J., & Nix, H. A. (1995). *Salinisation of Land and Water Resources: Human Causes, Extent, Management and Case Studies*. CAB International.

Ghermandi, A., Messalem, R., Offenbach, R., & Cohen, S. (2014). Solar desalination for sustainable brackish water management in arid land agriculture. *Renewable Agriculture and Food Systems*, *29*(3), 255–264. https://doi.org/10.1017/S1742170513000082

Goff, K., Lewis, M. E., Person, M. A., & Konikowd, L. F. (1998). Simulated Effects of Irrigation on Salinity in the Arkansas River Valley in Colorado. *Groundwater*, *36*(1), 76–86. https://doi.org/10.1111/j.1745-6584.1998.tb01067.x

Gojiya, K. M., Rank, H. D., Chauhan, P. M., Patel, D. V., Satasiya, R. M., & Prajapati, G. V. (2023). Remote Sensing and GIS Applications in Soil Salinity Analysis: A Comprehensive Review. *International Journal of Environment and Climate Change*, *13*(11), 2149–2161. https://doi.org/10.9734/ijecc/2023/v13i113377

Harrison, J. W., Lucius, M. A., Farrell, J. L., Eichler, L. W., & Relyea, R. A. (2021). Prediction of stream nitrogen and phosphorus concentrations from high-frequency sensors using Random Forests Regression. *Science of The Total Environment*, *763*, 143005. https://doi.org/10.1016/j.scitotenv.2020.143005

Ho, T. K. (1995). Random decision forests. *Proceedings of 3rd International Conference on Document Analysis and Recognition*, *1*, 278–282 vol.1. https://doi.org/10.1109/ICDAR.1995.598994

Jena, P. K., Rahaman, S. M., Das Mohapatra, P. K., Barik, D. P., & Patra, D. S. (2022). Surface water quality assessment by Random Forest. *Water Practice and Technology*, *18*(1), 201–214. https://doi.org/10.2166/wpt.2022.156

Jones, K. A., Niknami, L. S., Buto, S. G., & Decker, D. (2022). *Federal Standards and Procedures for the National Watershed Boundary Dataset (WBD) (5 ed.): U.S.*

Geological Survey Techniques and Methods 11-A3 (Techniques and Methods) [Techniques and Methods]. https://pubs.usgs.gov/tm/11/a3/

Kaner, A., Tripler, E., Hadas, E., & Ben-Gal, A. (2017). Feasibility of desalination as an alternative to irrigation with water high in salts. *Desalination*, *416*, 122–128. https://doi.org/10.1016/j.desal.2017.05.002

Khondoker, M., Mandal, S., Gurav, R., & Hwang, S. (2023). Freshwater Shortage, Salinity Increase, and Global Food Production: A Need for Sustainable Irrigation Water Desalination—A Scoping Review. *Earth*, *4*(2), Article 2. https://doi.org/10.3390/earth4020012

Knierim, K. J., Kingsbury, J. A., Haugh, C. J., & Ransom, K. M. (2020). Using Boosted Regression Tree Models to Predict Salinity in Mississippi Embayment Aquifers, Central United States. *JAWRA Journal of the American Water Resources Association*, *56*(6), 1010–1029. https://doi.org/10.1111/1752-1688.12879

Konikow, L. F., & Person, M. (1985). Assessment of Long-Term Salinity Changes in an Irrigated Stream-Aquifer System. *Water Resources Research*, *21*(11), 1611–1624. https://doi.org/10.1029/WR021i011p01611

Kumar, R., Ahmed, M., Bhadrachari, G., & Thomas, J. P. (2017). Desalination for agriculture: Water quality and plant chemistry, technologies and challenges. *Water Supply*, *18*(5), 1505–1517. https://doi.org/10.2166/ws.2017.229

Lin, Y., & Garcia, L. A. (2012). Assessing the Impact of Irrigation Return Flow on River Salinity for Colorado's Arkansas River Valley. *Journal of Irrigation and Drainage Engineering*, *138*(5), 406–415. https://doi.org/10.1061/(ASCE)IR.1943-4774.0000410

Melesse, A. M., Khosravi, K., Tiefenbacher, J. P., Heddam, S., Kim, S., Mosavi, A., & Pham, B. T. (2020). River Water Salinity Prediction Using Hybrid Machine Learning Models. *Water*, *12*(10), Article 10. https://doi.org/10.3390/w12102951

Metternicht, G. (2001). Assessing temporal and spatial changes of salinity using fuzzy logic, remote sensing and GIS. Foundations of an expert system. *Ecological Modelling*, *144*(2), 163–179. https://doi.org/10.1016/S0304-3800(01)00371-4

Mokhtar, A., Elbeltagi, A., Gyasi-Agyei, Y., Al-Ansari, N., & Abdel-Fattah, M. K. (2022). Prediction of irrigation water quality indices based on machine learning and regression models. *Applied Water Science*, *12*(4), 76. https://doi.org/10.1007/s13201-022-01590-x

Morway, E. D., & Gates, T. K. (2012). Regional Assessment of Soil Water Salinity across an Intensively Irrigated River Valley. *Journal of Irrigation and Drainage Engineering*, *138*(5), 393–405. https://doi.org/10.1061/(ASCE)IR.1943-4774.0000411

Munns, R. (2002). Comparative physiology of salt and water stress. *Plant, Cell & Environment*, *25*(2), 239–250. https://doi.org/10.1046/j.0016-8025.2001.00808.x

Musie, W., & Gonfa, G. (2023). Fresh water resource, scarcity, water salinity challenges and possible remedies: A review. *Heliyon*, *9*(8). https://doi.org/10.1016/j.heliyon.2023.e18685

Nasir, N., Kansal, A., Alshaltone, O., Barneih, F., Sameer, M., Shanableh, A., & Al-Shamma'a, A. (2022). Water quality classification using machine learning algorithms. *Journal of Water Process Engineering*, *48*, 102920. https://doi.org/10.1016/j.jwpe.2022.102920

Nouraki, A., Alavi, M., Golabi, M., & Albaji, M. (2021). Prediction of water quality parameters using machine learning models: A case study of the Karun River, Iran. *Environmental*

Science and Pollution Research, *28*(40), 57060–57072. https://doi.org/10.1007/s11356-021-14560-8

Osborn, B. (2019). *Lower Arkansas River Watershed Plan John Martin Reservoir to Stateline*. Colorado Department of Public Health and Environment (CDPHE). https://static1.squarespace.com/static/53f664ede4b032c1fade347d/t/5ed96cdcf038aa67b39bdab8/1591307537891/lower_arkansas_river_watershed_plan_john_martin_to_stateline_6.10.19_FINAL.pdf

Pedregosa, F., Varoquaux, G., Gramfort, A., Michel, V., Thirion, B., Grisel, O., Blondel, M., Prettenhofer, P., Weiss, R., Dubourg, V., Vanderplas, J., Passos, A., & Cournapeau, D. (2011). Scikit-learn: Machine Learning in Python. *MACHINE LEARNING IN PYTHON*, *12*, 2825–2830.

Read, E. K., Carr, L., De Cicco, L., Dugan, H. A., Hanson, P. C., Hart, J. A., Kreft, J., Read, J. S., & Winslow, L. A. (2017). Water quality data for national-scale aquatic research: The Water Quality Portal. *Water Resources Research*, *53*(2), 1735–1745. https://doi.org/10.1002/2016WR019993

Shams, M. Y., Elshewey, A. M., El-kenawy, E.-S. M., Ibrahim, A., Talaat, F. M., & Tarek, Z. (2024). Water quality prediction using machine learning models based on grid search method. *Multimedia Tools and Applications*, *83*(12), 35307–35334. https://doi.org/10.1007/s11042-023-16737-4

Slater, Y., Finkelshtain, I., Reznik, A., & Kan, I. (2020). Large-Scale Desalination and the External Impact on Irrigation-Water Salinity: Economic Analysis for the Case of Israel. *Water Resources Research*, *56*(9), e2019WR025657. https://doi.org/10.1029/2019WR025657

Stanton, J. S., Anning, D. W., Brown, C. J., Moore, R. B., McGuire, V. L., Qi, S. L., Harris, A. C., Dennehy, K. F., McMahon, P. B., Degnan, J. R., & Böhlke, J. K. (2017). Brackish groundwater in the United States. In *Professional Paper* (1833). U.S. Geological Survey. https://doi.org/10.3133/pp1833

Suri, M., Betak, J., Rosina, K., Chrkavy, D., Suriova, N., Cebecauer, T., Caltik, M., & Erdelyi, B. (2020, June). *Global Photovoltaic Power Potential by Country* [Text/HTML]. World Bank. https://documents.worldbank.org/en/publication/documents-reports/documentdetail/466331592817725242/Global-Photovoltaic-Power-Potential-by-Country

Syner, J. P. (1987). *Map Projections—A Working Manual* (U.S. GEOLOGICAL SURVEY PROFESSIONAL PAPER 1395). U.S. GEOLOGICAL SURVEY. https://pubs.usgs.gov/pp/1395/report.pdf

Thorslund, J., Bierkens, M. F. P., Oude Essink, G. H. P., Sutanudjaja, E. H., & van Vliet, M. T. H. (2021). Common irrigation drivers of freshwater salinisation in river basins worldwide. *Nature Communications*, *12*(1), 4232. https://doi.org/10.1038/s41467-021-24281-8

Thorslund, J., & van Vliet, M. T. H. (2020). A global dataset of surface water and groundwater salinity measurements from 1980–2019. *Scientific Data*, *7*(1), 231. https://doi.org/10.1038/s41597-020-0562-z

Tyralis, H., Papacharalampous, G., & Langousis, A. (2019). A Brief Review of Random Forests for Water Scientists and Practitioners and Their Recent History in Water Resources. *Water*, *11*(5), Article 5. https://doi.org/10.3390/w11050910

Wetzel, R. G. (2001). 10—SALINITY OF INLAND WATERS. In R. G. Wetzel (Ed.), *Limnology (Third Edition)* (pp. 169–186). Academic Press. https://doi.org/10.1016/B978-0-08-057439-4.50014-9

Wind Energy Factsheet | Center for Sustainable Systems. (2024). https://css.umich.edu/publications/factsheets/energy/wind-energy-factsheet

Wiser, R., Bolinger, M., Hoen, B., Millstein, D., Rand, J., Barbose, G., Darghouth, N., Gorman, W., Jeong, S., O'Shaughnessy, E., & Paulos, B. (2023). *Land-Based Wind Market Report: 2023 Edition*.

Xie, Y., & Lark, T. J. (2021). Mapping annual irrigation from Landsat imagery and environmental variables across the conterminous United States. *Remote Sensing of Environment*, *260*, 112445. https://doi.org/10.1016/j.rse.2021.112445

Yermiyahu, U., Tal, A., Ben-Gal, A., Bar-Tal, A., Tarchitzky, J., & Lahav, O. (2007). Rethinking Desalinated Water Quality and Agriculture. *Science*, *318*(5852), 920–921. https://doi.org/10.1126/science.1146339